European Journal of Control 72 (2023) 100828

Contents lists available at ScienceDirect

European Journal of Control

journal homepage: www.elsevier.com/locate/ejcon

# Energy shaping control of a class of underactuated mechanical systems with high-order actuator dynamics

Enrico Franco[a,*], Alessandro Astolfi[b,c]

[a] Mechanical Engineering Department, Imperial College London, London SW72AZ, UK
[b] Electrical and Electronic Engineering Department, Imperial College London, London SW72AZ, UK
[c] Dipartimento di Ingegneria Civile e Ingegneria Informatica, Universitá di Roma "Tor Vergata", Rome 00133, Italy

ARTICLE INFO

*Article history:*
Received 4 November 2022
Revised 23 February 2023
Accepted 5 May 2023
Available online 11 May 2023

Recommended by Prof. T Parisini

*Keywords:*
Underactuated mechanical systems
Actuator dynamics
Energy shaping
Nonlinear systems

ABSTRACT

In this work we present some new results on energy shaping control for underactuated mechanical systems with high-order actuator dynamics. To this end, we propose an extension of the *Interconnection and damping assignment Passivity based control* methodology to account for actuator dynamics. This brings the following new results: i) a potential and kinetic energy shaping and damping assignment procedure that yields two alternative controllers; ii) a potential energy shaping and damping assignment procedure for a narrower class of underactuated mechanical systems. The proposed approach is illustrated with numerical simulations on three examples: an Acrobot system with a series elastic actuator; a soft continuum manipulator actuated by electroactive polymers; a two-mass-spring system actuated by a DC motor.



## 1. Introduction

Energy shaping control offers a range of desirable features, including the physical interpretation of the control action in terms of system energy, which have made this approach a popular choice for a variety of applications. In particular, the *Interconnection and damping assignment Passivity based control* (IDA-PBC) methodology [18] involves designing the control action such that the closed-loop dynamics preserves the port-Hamiltonian structure and is characterized by a prescribed total energy. IDA-PBC controllers have been designed for a variety of systems, including fully actuated robots [23], underactuated satellites [2], unmanned surface vessels [14,20], piezoelectric beams [12], and soft robotic manipulators [7,15]. In case of underactuated systems, the controller design requires solving analytically a set of partial differential equations (PDEs), which can be a challenging task. This aspect has motivated a number of works, including a method to simplify the PDEs for mechanical systems [21], the study of kinetic energy shaping for mechanical systems [11], the algebraic solutions of the PDEs in Nunna et al. [17], and the numerical solution of the PDEs with reinforcement learning in Gheibi et al. [10]. A further line of research has investigated the effect of disturbances within IDA-PBC, resulting in more sophisticated controllers that achieve robustification through integral actions [3] or adaptive observers [8].

Thanks to its physical interpretation in terms of system energy, the IDA-PBC methodology has proved well suited to control multi-domain systems which involve energy exchanges between different components. Notable examples include magnetic levitation systems [17], weakly-coupled electro-mechanical systems [22], and more recently mechanical systems with fluidic actuation [5,6]. In principle, the IDA-PBC methodology can be employed to account for high-order actuator dynamics within the controller design. Nevertheless, this has typically been avoided for simplicity, considering that many actuators have higher bandwidth compared to the corresponding mechanical sub-systems [19]. In general, accounting for the actuator dynamics results in a system which is not input affine hence potentially complicating the controller design. Notable results in this direction include IDA-PBC designs for mechanical systems that account for the first-order dynamics of electric motors in Gandarilla et al. [9] and Wang et al. [26]. In addition, an energy shaping controller has been designed for a soft continuum manipulator actuated by electroactive polymers in Mattioni et al. [15]. Finally, in our recent work [5], we have proposed an IDA-PBC implementation for underactuated mechanical systems with fluidic actuation, which accounts for the pressure dynamics of the fluid, either pneumatic or hydraulic. In summary, the former controllers are either specific to a system or to a type of actuator, thus they are not directly applicable to different actuation strategies characterized by high-order dynamics.

* Corresponding author.
*E-mail address:* e.franco11@imperial.ac.uk (E. Franco).

https://doi.org/10.1016/j.ejcon.2023.100828

This work investigates the energy shaping control for underactuated mechanical system with high-order actuator dynamics and presents the following new results.

- An energy shaping and damping assignment procedure that builds upon the IDA-PBC methodology preserving the port-Hamiltonian structure, and which yields two alternative controllers. This approach is feasible for a class of systems defined by a clear set of conditions. In addition, a potential shaping procedure is detailed for a narrower class of underactuated mechanical systems.
- Numerical simulations for three illustrative case studies: an Acrobot system with a series elastic actuator; a soft continuum manipulator actuated by electroactive polymers; a two-mass-spring system actuated by a DC motor.

The rest of this paper is organized as follows: a brief overview of the IDA-PBC methodology is provided in Section 2 for completeness; the definition of the system class is given in Section 3; two controller design procedures for kinetic and potential energy shaping are detailed in Section 4; a controller design procedure for potential energy shaping is discussed in Section 5; illustrative examples are presented in Section 6; concluding remarks are given in Section 7.

## 2. Overview of IDA-PBC

The dynamics of an underactuated mechanical system with $n$ degrees-of-freedom (DOFs) and direct actuation $u \in \mathbb{R}^m$ through the input matrix $G(q) \in \mathbb{R}^{n\times m}$, where $\mathrm{rank}(G) = m < n$ for all $q \in \mathbb{R}^n$, is described in port-Hamiltonian form as

$$\begin{bmatrix}\dot q\\ \dot p\end{bmatrix} = \begin{bmatrix}0 & I\\ -I & -D\end{bmatrix}\begin{bmatrix}\nabla_q H\\ \nabla_p H\end{bmatrix} + \begin{bmatrix}0\\ G\end{bmatrix}u,\ \ y = G^T\nabla_p H, \tag{1}$$

where $D = D^T \geq 0$ is the damping matrix, and the total mechanical energy is

$$H(q,p) = \Omega + \frac{1}{2}p^T M^{-1} p, \tag{2}$$

characterized by the inertia matrix $M(q) = M(q)^T > 0$, and the potential energy $\Omega(q)$. The system states are the position $q \in \mathbb{R}^n$ and the momenta $p = M\dot q \in \mathbb{R}^n$. The remaining terms in (1) are the identity matrix $I$, the vector of partial derivatives of $H$ in $q$, $\nabla_q H$, and the vector of partial derivatives of $H$ in $p$, $\nabla_p H$. The control aim corresponds to stabilizing the equilibrium $(q,p) = (q^*, 0)$, and it is achieved with the IDA-PBC control law [18]

$$u = G^\dagger\left(\nabla_q H - M_d M^{-1}\nabla_q H_d + J_2\nabla_p H_d\right) - k_v G^T\nabla_p H_d, \tag{3}$$

where $G^\dagger = \left(G^T G\right)^{-1}G^T$. The resulting closed-loop dynamics is

$$\begin{bmatrix}\dot q\\ \dot p\end{bmatrix} = \begin{bmatrix}0 & M^{-1}M_d\\ -M_d M^{-1} & J_2 - (Gk_vG^T + DM^{-1}M_d)\end{bmatrix}\begin{bmatrix}\nabla_q H_d\\ \nabla_p H_d\end{bmatrix} \tag{4}$$

where $H_d = \Omega_d + \frac{1}{2}p^T M_d^{-1}p$. The design parameters in (4) are the potential energy $\Omega_d$, the inertia matrix $M_d = M_d^T > 0$, the free matrix $J_2 = -J_2^T$, and the constant matrix $k_v = k_v^T > 0$. To achieve the regulation goal, the potential energy $\Omega_d$ should admit a strict global minimizer in $q^*$ hence verifying the conditions $\nabla_q\Omega_d(q^*) = 0$ and $\nabla_q^2\Omega_d(q^*) > 0$. In addition, $M_d$ and $\Omega_d$ should verify for all $(q,p) \in \mathbb{R}^{2n}$ the PDEs

$$G^\perp\left(\nabla_q(p^T M^{-1}p) - M_d M^{-1}\nabla_q(p^T M_d^{-1}p) + 2J_2 M_d^{-1}p\right) = 0, \tag{5}$$

$$G^\perp\left(\nabla_q\Omega - M_d M^{-1}\nabla_q\Omega_d\right) = 0, \tag{6}$$

where $G^\perp$ is such that $G^\perp G = 0$ and $\mathrm{rank}\left(G^\perp\right) = n - m$. Computing the time derivative of $H_d$ along the trajectories of the closed-loop system (4) yields

$$\dot H_d = -\nabla_p H_d^T\left(Gk_vG^T + \frac{1}{2}(DM^{-1}M_d) + \frac{1}{2}(DM^{-1}M_d)^T\right)\nabla_p H_d \leq 0. \tag{7}$$

Thus the equilibrium $(q,p) = (q^*, 0)$ is asymptotically stable if $\left(Gk_vG^T + \frac{1}{2}(DM^{-1}M_d) + \frac{1}{2}(DM^{-1}M_d)^T\right) \geq 0$ and the output $y = G^T\nabla_p H_d$ is detectable [18].

## 3. System class definition

Consider the underactuated mechanical system defined by (1) and (2) where the actuator dynamics has order $s \geq 1$. The complete system dynamics in port-Hamiltonian form is thus

$$\begin{bmatrix}\dot q\\ \dot p\\ \dot x_1\\ \dot x_2\\ \dots\\ \dot x_s\end{bmatrix} = \underbrace{\begin{bmatrix}0 & I & 0 & 0 & \dots & 0\\ -I & -D & \mathcal{F}_{23} & 0 & \dots & 0\\ 0 & -\mathcal{F}_{23}^T & -\mathcal{R}_{33} & \mathcal{F}_{34} & \dots & 0\\ 0 & 0 & -\mathcal{R}_{34}^T & -\mathcal{R}_{44} & \dots & 0\\ \dots & \dots & \dots & \dots & \dots & \dots\\ 0 & 0 & 0 & 0 & \dots & -\mathcal{R}_{s+2,s+2}\end{bmatrix}}_{\mathcal{F}}$$

$$\begin{bmatrix}\nabla_q W\\ \nabla_p W\\ \nabla_{x_1} W\\ \nabla_{x_2} W\\ \dots\\ \nabla_{x_s} W\end{bmatrix} + \begin{bmatrix}0\\ 0\\ 0\\ 0\\ \dots\\ G_0\end{bmatrix}u, \tag{8}$$

where $W = \Omega + \frac{1}{2}p^T M^{-1}p + \sum_{j=1}^s E_j$ and $\mathcal{F} = \mathcal{F}_0 - \mathcal{R}_0$ with $\mathcal{F}_0 = -\mathcal{F}_0^T$, $\mathcal{R}_0 = \mathcal{R}_0^T = \mathrm{diag}(\mathcal{R}_{ii})$. The generic element of $\mathcal{F}$ on row $i$ and column $j$ is indicated with $\mathcal{F}_{ij}$, thus $\mathcal{F}_{ji} = -\mathcal{F}_{ij}$ for all $i \neq j$. In summary, the total energy $W$ comprises the mechanical energy $H = \Omega + \frac{1}{2}p^T M^{-1}p$, while the remaining terms $E_j$ represent the energy of the actuators. The system states are $x = (q, p, x_1, \dots, x_s)$ with $q \in \mathbb{R}^n$, $p \in \mathbb{R}^n$ referring to the mechanical system (1), and $(x_1, \dots, x_s) \in \mathbb{R}^{m\times s}$ referring to the actuator, and the new input matrix is $G_0 \in \mathbb{R}^{m\times m}$. In summary, system (8) is an extension of system (1) obtained by including the dynamics of the actuators. The class of systems considered in this work is defined by the following assumptions.

**Assumption 1.** The PDEs (5) and (6) for system (1) with direct actuation are solvable analytically, $\Omega_d$ is positive definite, $q^* = \mathrm{argmin}(\Omega_d)$, and either $D_d = Gk_vG^T + \frac{1}{2}(DM^{-1}M_d) + \frac{1}{2}(DM^{-1}M_d)^T > 0$, or $y = G^T M_d^{-1}p$ is detectable if $D = 0$. Finally, all model parameters are exactly known and all system states are measurable.

**Assumption 2.** The interconnection matrix $\mathcal{F}$ in (8) has off-diagonal elements $\mathcal{F}_{ij} = 0$ if $j > i+1$ and either $\mathrm{rank}(\mathcal{F}_{ij}) = m$ if $j = i+1$ or $\nabla_{x_j}\left(\mathcal{F}_{j+1,1}^T\nabla_q W + \mathcal{F}_{j+1,2}\nabla_p W\right) \neq 0$, while the diagonal terms are $\mathcal{R}_{ii} \geq 0$.

**Assumption 3.** The energy of the actuators is such that $\nabla_{x_j}E_i = 0$ if $j > i$ and $\nabla_{x_j}E_j \neq 0$. Finally, $G_0$ is full rank for all $(q, p, x_1, \dots, x_s)$.

**Remark 1.** The first assumption defines the class of systems for which the IDA-PBC methodology is applicable, according to Ortega et al. [18]. The analytical solvability of the PDEs is a research topic in itself [17], thus it is not investigated further. Nevertheless, the PDEs (5) and (6) are solvable analytically for several canonical examples including, the disk-on-disk [3], the inertia-wheel-pendulum [21], the ball-on-beam [18], and the Acrobot [16], which is illustrated in Section 6. If $s = 0$ the conditions of

Assumptions 2 and 3 are verified, that is $\mathcal{F}_{12} = I \neq 0$, $\mathcal{R}_{22} = D \geq 0$ and $\nabla_p \Omega = 0$, $\nabla_q^2 \Omega \neq 0$, $\nabla_p^2 \left(\frac{1}{2} p^T M^{-1} p\right) = M^{-1} \neq 0$. In general, Assumptions 2 and 3 imply that the actuator dynamics in (8) is in strict-feedback form, with the key difference that the mechanical sub-system (1) is underactuated. As a result, the controller design cannot be performed with the same backstepping approach used for fully actuated systems [13]. In addition, employing a backstepping design that builds upon the IDA-PBC controller (3) would not preserve the port-Hamiltonian structure in closed loop [5,6]. Note finally that, while systems (8) is not directly actuated, the input matrix $G$ is still relevant since it defines the states affected by the actuator dynamics.

## 4. Potential and kinetic energy shaping

The aim of this work is to account for high-order actuator dynamics by building upon the IDA-PBC methodology [18] in a modular fashion and by preserving the port-Hamiltonian structure of the system in closed loop. To this end we propose a controller design procedure that preserves the PDEs (5) and (6) characterizing system (1). The main idea behind the controller design is to: i) express the actuator dynamics in port-Hamiltonian form (8); ii) define a corresponding closed-loop dynamics compatibly with the regulation goal; iii) construct a control law that ensures matching between open-loop and closed-loop dynamics thus extending our work [5] to generic high-order actuator dynamics.

### 4.1. First controller design

The control law for system (8) is designed such that the closed-loop dynamics is port-Hamiltonian, that is

$$\left[\dot{x}\right] = \left[\mathcal{F}'\right]\left[\nabla_x W_d\right], \tag{9}$$

where $\mathcal{F}' = \mathcal{F}^* - \mathcal{R}^*$ with $\mathcal{F}^* = -\mathcal{F}^{*T}$ and $\mathcal{R}^* = \mathcal{R}^{*T} \geq 0$, the total energy is $W_d = H_d + \frac{1}{2}\sum_{k=1}^{s} \zeta_k^T \zeta_k$, with $H_d = \Omega_d + \frac{1}{2} p^T M_d^{-1} p$ characterizing the mechanical sub-system, and $\zeta_k \in \mathbb{R}^m$ are defined as

$$\zeta_k = \begin{cases} G^\dagger\left(-\nabla_q W + \mathcal{F}_{23}\nabla_{x_1} W + M_d M^{-1}\nabla_q H_d + \left(G k_v G^T - J_2\right)\nabla_p H_d\right), & k = 1 \\ -\mathcal{F}_{2,k+1}^T \nabla_p W - \sum_{j=1}^{k} \mathcal{F}_{j+2,k+1}^T \nabla_{x_j} W + \mathcal{F}_{1,k+1}^{'T}\left(\nabla_q H_d + \sum_{i=1}^{k-1}(\nabla_q \zeta_i)^T \zeta_i\right) & \\ +\mathcal{F}_{2,k+1}^{'T}\left(\nabla_p H_d + \sum_{i=1}^{k-1}(\nabla_p \zeta_i)^T \zeta_i\right) + \sum_{j=1}^{k-1} \mathcal{F}_{j+2,k+1}^{'T}\left(\sum_{i=1}^{k-1}(\nabla_{x_j}\zeta_i)^T \zeta_i\right), & k > 1, \end{cases} \tag{10}$$

to ensure matching between (8) and (9) for the states $(x_1, \ldots, x_s)$. The elements of $\mathcal{F}'$ on or above the diagonal (i.e., $\mathcal{F}'_{kj}$ on row $k$ and column $j \geq k$), are defined as

$$\begin{aligned} &\mathcal{F}'_{11} = 0,\ \mathcal{F}'_{12} = M^{-1}M_d,\ \mathcal{F}'_{22} = -DM^{-1}M_d - G k_v G^T + J_2, \\ &\mathcal{F}'_{23} = G\left(1 + G^\dagger \mathcal{F}_{12}^{'T}\nabla_q \zeta_1 - G^\dagger \mathcal{F}'_{22}\nabla_p \zeta_1\right)(\nabla_{x_1}\zeta_1)^{-1} + G^{\perp^T}\left(G^{\otimes}\mathcal{F}_{12}^{'T}\nabla_q\zeta_1 - G^{\otimes}\mathcal{F}'_{22}\nabla_p\zeta_1\right)(\nabla_{x_1}\zeta_1)^{-1}, \\ &\mathcal{F}'_{kj} = \begin{cases} \left(1 + \mathcal{F}_{1k}^{'T}\nabla_q\zeta_{j-2} + \mathcal{F}_{2k}^{'T}\nabla_p\zeta_{j-2} + \sum_{i=3}^{j-1}\left(\mathcal{F}_{ik}^{'T}\nabla_{x_{i-2}}\zeta_{j-2}\right)\right)\left(\nabla_{x_{j-2}}\zeta_{j-2}\right)^{-1} & j = k+1 > 3 \\ \left(\mathcal{F}_{1k}^{'T}\nabla_q\zeta_{j-2} + \mathcal{F}_{2k}^{'T}\nabla_p\zeta_{j-2} + \sum_{i=3}^{j-1}\left(\mathcal{F}_{ik}^{'T}\nabla_{x_{i-2}}\zeta_{j-2}\right)\right)\left(\nabla_{x_{j-2}}\zeta_{j-2}\right)^{-1} & j > k+1, \\ -K_{j-2} < 0 & j = k > 2, \end{cases} \end{aligned} \tag{11}$$

where $G^{\otimes} = (G^\perp G^{\perp^T})^{-1}G^\perp$, $K_{j-2}$ are tuning parameters, while $\Omega_d, M_d$ and $J_2$ are computed by solving the PDEs (5) and (6) that characterize system (1). It follows from (10) that $\nabla_{x_1}\zeta_1 = G^\dagger \mathcal{F}_{23}\nabla_{x_1}E_1$, where $\mathrm{rank}(\mathcal{F}_{23}) = m$ (see Assumption 2) and $\nabla_{x_1}E_1 \neq 0$ (see Assumption 3) hence $\mathrm{rank}(\nabla_{x_1}\zeta_1) = m$. The same applies to $\nabla_{x_j}\zeta_j$. The control input that yields the closed-loop dynamics (9) is

$$u = G_0^{-1}\left(\mathcal{F}_{1,s+2}^T\nabla_q W + \mathcal{F}_{2,s+2}^T\nabla_p W + \sum_{j=1}^{s}\mathcal{F}_{j+2,s+2}^T\nabla_{x_j}W - \mathcal{F}_{1,s+2}^{'T}\nabla_q W_d - \mathcal{F}_{2,s+2}^{'T}\nabla_p W_d - \sum_{j=1}^{s}\mathcal{F}_{j+2,s+2}^{'T}\nabla_{x_j}W_d\right). \tag{12}$$

It follows from (10), (11) that $\zeta_k$ and $\mathcal{F}'_{kj}$ are interdependent, thus they cannot be computed simultaneously and independently of each other. Therefore, the control law is constructed by employing the following design procedure.

1. Compute the expressions of $\Omega_d, M_d$ and $J_2$ by solving the PDEs (5) and (6) for the mechanical sub-system (1).
2. Compute $\mathcal{F}'_{12}, \mathcal{F}'_{22}$ and the diagonal terms $\mathcal{F}'_{jj}$ from (11).
3. Compute $\zeta_1$ from (10) and subsequently compute $\mathcal{F}'_{13}, \mathcal{F}'_{23}$ from (11).
4. Compute $\zeta_2$ from (10) and subsequently compute $\mathcal{F}'_{14}, \mathcal{F}'_{24}, \mathcal{F}'_{34}$ from (11).
5. Compute $\zeta_k$ from (10) and subsequently compute $\mathcal{F}'_{1,k+2}, \mathcal{F}'_{2,k+2}, \ldots, \mathcal{F}'_{k+1,k+2}$ from (11) for all subsequent $k \leq s$.
6. Compute the control input from (12).

**Proposition 1.** *Consider system (8) with Assumptions 1–3 and with the control law (12). Then the closed-loop system is given by (9), the matrix $\mathcal{F}'$ is given by (11), and $\zeta_k$ is given by (10).*

**Proof.** Equating the first rows in (8) and (9) yields

$$M^{-1}p = M^{-1}M_d\left(M_d^{-1}p + \sum_{k=1}^{s}(\nabla_p\zeta_k)^T\zeta_k\right) + \sum_{j=1}^{s}\left(\mathcal{F}'_{1,j+2}\sum_{k=j}^{s}(\nabla_{x_j}\zeta_k)^T\zeta_k\right). \tag{13}$$

Defining $\mathcal{F}'_{1,s+2}$ according to (11), that is

$$\mathcal{F}'_{1,s+2} = -\left(\mathcal{F}'_{12}\nabla_p\zeta_s + \sum_{j=1}^{s-1}\left(\mathcal{F}'_{1,j+2}\nabla_{x_j}\zeta_s\right)\right)(\nabla_{x_s}\zeta_s)^{-1},$$

and substituting in (13) cancels $\zeta_s$. Similarly, substituting $\mathcal{F}'_{1,j+2}$ with $j > 2$ cancels $\zeta_j$ until (13) yields the identity.

Equating the second rows in (8) and (9) yields

$$-\nabla_q W - DM^{-1}p + \mathcal{F}_{23}\nabla_{x_1}W = -\mathcal{F}_{12}^{'T}\left(\nabla_q H_d + \sum_{k=1}^{s}(\nabla_q\zeta_k)^T\zeta_k\right) + \mathcal{F}_{22}^{'}\left(M_d^{-1}p + \sum_{k=1}^{s}(\nabla_p\zeta_k)^T\zeta_k\right) + \sum_{j=1}^{s}\left(\mathcal{F}_{2,j+2}^{'}\sum_{k=j}^{s}(\nabla_{x_j}\zeta_k)^T\zeta_k\right). \quad (14)$$

Defining $\mathcal{F}_{2,j+2}^{'}$ with $j>1$ according to (11) and substituting it in (14) cancels $\zeta_j$ for all $j>1$. Substituting $\mathcal{F}_{22}^{'}$ while simplifying common terms, and pre-multiplying both sides of (14) by $G^{\otimes}$ gives the matching conditions [5]

$$G^{\otimes}\left(-\nabla_q H + \mathcal{F}_{12}^{'T}\nabla_q H_d - J_2 M_d^{-1}p\right) = G^{\otimes}\left(-\mathcal{F}_{12}^{'T}(\nabla_q\zeta_1)^T\zeta_1 + \mathcal{F}_{22}^{'}(\nabla_p\zeta_1)^T\zeta_1 + \mathcal{F}_{23}^{'}(\nabla_{x_1}\zeta_1)^T\zeta_1\right), \quad (15)$$

where the left side of the equal corresponds to the sum of the PDEs (5) and (6) (solvable analytically by hypothesis according to Assumption 1). Thus PDEs (5) and (6) are preserved as well as their analytical solutions $\Omega_d$, $M_d$ and $J_2$. Note that $\mathcal{F}_{23}\nabla_{x_1}W$ is not part of (15), since it only affects the actuated states of the mechanical system (i.e., the actuator dynamics enters the system through the matrix $G$). Pre-multiplying both sides of (14) by $G^{\dagger}$ yields instead

$$G^{\dagger}\left(-\nabla_q W + \mathcal{F}_{23}\nabla_{x_1}W + \mathcal{F}_{12}^{'T}\nabla_q H_d + \left(Gk_vG^T - J_2\right)M_d^{-1}p\right) = G^{\dagger}\left(-\mathcal{F}_{12}^{'T}(\nabla_q\zeta_1)^T\zeta_1 + \mathcal{F}_{22}^{'}(\nabla_p\zeta_1)^T\zeta_1 + \mathcal{F}_{23}^{'}(\nabla_{x_1}\zeta_1)^T\zeta_1\right), \quad (16)$$

where the terms to the left of the equal correspond to $\zeta_1$ in (10). Note that $\nabla_{x_j}\zeta_1 = 0$ for all $j>1$. Thus, defining $\mathcal{F}_{23}^{'}$ according to (11) solves both (15) and (16).

Equating the third rows in (8) and (9) yields

$$-\mathcal{F}_{23}^{T}\nabla_p W - \mathcal{F}_{33}\nabla_{x_1}W + \mathcal{F}_{34}\nabla_{x_2}W = -\mathcal{F}_{13}^{'T}\left(\nabla_q H_d + \sum_{k=1}^{s}(\nabla_q\zeta_k)^T\zeta_k\right) - \mathcal{F}_{23}^{'T}\left(M_d^{-1}p + \sum_{k=1}^{s}(\nabla_p\zeta_k)^T\zeta_k\right) + \sum_{j=1}^{s}\left(\mathcal{F}_{3,j+2}^{'}\sum_{k=j}^{s}(\nabla_{x_j}\zeta_k)^T\zeta_k\right). \quad (17)$$

Defining $\mathcal{F}_{3,j+2}^{'}$ with $j>2$ according to (11) and substituting it in (17) cancels $\zeta_j$ for all $j>2$ yielding

$$\begin{aligned}&-\mathcal{F}_{23}^{T}\nabla_p W - \mathcal{F}_{33}\nabla_{x_1}W + \mathcal{F}_{34}\nabla_{x_2}W\\ &+\mathcal{F}_{13}^{'T}\left(\nabla_q H_d + (\nabla_q\zeta_1)^T\zeta_1\right) + \mathcal{F}_{23}^{'T}\left(M_d^{-1}p + (\nabla_p\zeta_1)^T\zeta_1\right)\\ &-\mathcal{F}_{33}^{'}\left((\nabla_{x_1}\zeta_1)^T\zeta_1\right) =\\ &-\mathcal{F}_{13}^{'T}\left((\nabla_q\zeta_2)^T\zeta_2\right) - \mathcal{F}_{23}^{'T}\left((\nabla_p\zeta_2)^T\zeta_2\right)\\ &+\mathcal{F}_{33}^{'}(\nabla_{x_1}\zeta_2)^T\zeta_2 + \mathcal{F}_{34}^{'}(\nabla_{x_2}\zeta_2)^T\zeta_2. \end{aligned} \quad (18)$$

The terms to the left of the equal correspond to $\zeta_2$, where $\nabla_{x_j}\zeta_2 = 0$ for all $j>2$. Thus (18) is verified by defining $\mathcal{F}_{34}^{'}$ as in (11), that is

$$\mathcal{F}_{34}^{'} = \left(1 + \mathcal{F}_{13}^{'T}\nabla_q\zeta_2 + \mathcal{F}_{23}^{'T}\nabla_p\zeta_2 - \mathcal{F}_{33}^{'}\nabla_{x_1}\zeta_2\right)(\nabla_{x_2}\zeta_2)^{-1}$$

Matching for the remaining states $x_j$ with $j<s$ is achieved in the same fashion and is omitted for conciseness.

Equating the last rows in (8) and (9) yields finally

$$-\mathcal{F}_{1,s+2}^{T}\nabla_q W - \mathcal{F}_{2,s+2}^{T}\nabla_p W - \sum_{j=1}^{s}\mathcal{F}_{j+2,s+2}^{T}\nabla_{x_j}W + G_0u = -\mathcal{F}_{1,s+2}^{'T}\left(\nabla_q H_d + \sum_{k=1}^{s}(\nabla_q\zeta_k)^T\zeta_k\right) - \mathcal{F}_{2,s+2}^{'T}\left(M_d^{-1}p + \sum_{k=1}^{s}(\nabla_p\zeta_k)^T\zeta_k\right) - \sum_{j=1}^{s}\left(\mathcal{F}_{j+2,s+2}^{'T}\sum_{k=j}^{s}(\nabla_{x_j}\zeta_k)^T\zeta_k\right). \quad (19)$$

Computing $u$ from (19) yields (12) concluding the proof. □

**Remark 2.** In summary, the proposed design procedure results in the same PDEs as the traditional IDA-PBC [18]. It follows from Assumptions 2 and 3 that $\nabla_{x_j}\zeta_i = 0,\ \forall j>i$ and that $\nabla_{x_j}\zeta_j \neq 0$, thus $\mathcal{F}_{k,j}^{'} \in \mathcal{L}^{\infty}$. If the terms $\mathcal{F}_{j,j+1}$ are constant, Assumption 2 is verified provided that $\nabla_{x_j}^2 E_j \neq 0,\ \forall j$. If instead Assumptions 2 and 3 are not verified, that is for instance $\mathcal{F}_{14}\nabla_{x_2}W \neq 0$, then it follows from (16) that $\zeta_1$ would depend also on $x_2$. Consequently, choosing $\mathcal{F}_{13}^{'}$ to verify (13) would yield

$$\mathcal{F}_{13}^{'} = -\left(\mathcal{F}_{12}^{'}\nabla_p\zeta_1 + \mathcal{F}_{14}^{'}\nabla_{x_2}\zeta_1\right)(\nabla_{x_1}\zeta_1)^{-1},$$

which also contains $\mathcal{F}_{14}^{'}$. However, it follows from (11) that $\mathcal{F}_{14}^{'}$ depends on $\mathcal{F}_{13}^{'}$ thus the design procedure outlined in Proposition 1 would not be feasible in such case.

**Proposition 2.** *Consider system (8) with Assumptions 1 to 3, in closed-loop with the control law (12). Then the equilibrium $x=x^*$, with $q=q^*$ and $p=p^*=0$, is asymptotically stable for all $K_j>0$ provided that either $(Gk_vG^T + \frac{1}{2}(DM^{-1}M_d) + \frac{1}{2}(DM^{-1}M_d)^T) > 0$, or that $D=0$ and the output $y=G^TM_d^{-1}p$ is detectable.*

**Proof.** Note first that $W_d = \Omega_d + \frac{1}{2}p^TM_d^{-1}p + \frac{1}{2}\sum_{k=1}^{s}\zeta_k^T\zeta_k$ is positive definite. Expressing $(DM^{-1}M_d)$ as the sum of a symmetric part $\Phi_0$ and an antisymmetric part $\Psi_0$, that is $(DM^{-1}M_d) = \Phi_0 + \Psi_0$, where $\Phi_0 = \frac{1}{2}(DM^{-1}M_d) + \frac{1}{2}(DM^{-1}M_d)^T$ and $\Psi_0 = \frac{1}{2}(DM^{-1}M_d) - \frac{1}{2}(DM^{-1}M_d)^T$, and computing the time derivative of $W_d$ along the trajectories of the closed-loop system (9) while recalling that $J_2 = -J_2^T$ yields

$$\dot{W}_d = -\nabla_p W_d^T\left(Gk_vG^T + \Phi_0\right)\nabla_p W_d - \sum_{j=1}^{s}\left(\nabla_{x_j}W_d^TK_j\nabla_{x_j}W_d\right) \le 0, \quad (20)$$

where $\nabla_p W_d = M_d^{-1}p + \sum_{j=i}^{s}((\nabla_p\zeta_j)^T\zeta_j)$, $\nabla_{x_i}W_d = \sum_{j=i}^{s}((\nabla_{x_i}\zeta_j)^T\zeta_j)$, and $\nabla_{x_s}W_d = (\nabla_{x_s}\zeta_s)^T\zeta_s$. If $K_j>0, D\neq 0$ and $(Gk_vG^T + \Phi_0) > 0$ it follows from (20) that $q, p, \zeta_j \in \mathcal{L}^{\infty}, \forall j$, while $p, \sum_{j=i}^{s}((\nabla_{x_i}\zeta_j)^T\zeta_j), \zeta_s \in \mathcal{L}^2$. It follows from (10) that $\nabla_{x_j}\zeta_j \neq 0$, thus $p, \zeta_j \in \mathcal{L}^2 \cap \mathcal{L}^{\infty}, \forall j$. Finally, it follows from (9) that $\dot{q}, \dot{p}, \dot{\zeta}_j \in \mathcal{L}^{\infty}$. Thus $\zeta_j, p$ converge to zero asymptotically according to Barbalat's Lemma, and the equilibrium is asymptotically stable [24]. In case $D=0$, it follows from (20) that $y \in \mathcal{L}^2 \cap \mathcal{L}^{\infty}$ and from (9) that $\dot{q}, \dot{p} \in \mathcal{L}^{\infty}$ hence also $\dot{y} \in \mathcal{L}^{\infty}$, and $y$ converges to zero asymptotically rather than $p$. Asymptotic stability of the equilibrium is then established in a similar fashion, provided that the output $y = G^TM_d^{-1}p$ is detectable [18].

Substituting $\dot{p} = p = 0$ and $\zeta_j = 0$ in (9) yields $\nabla_q\Omega_d = 0$, thus the equilibrium is an extremum of $\Omega_d$, while $\nabla_q^2\Omega_d(q^*) > 0$ by design, that is $q^* = \mathrm{argmin}(\Omega_d)$. Substituting $p=0$ and $\zeta_j = 0$ in (10) yields

$$\begin{aligned}&G^{\dagger}\left(-\nabla_q\Omega + \mathcal{F}_{23}\nabla_{x_1}W + M_dM^{-1}\nabla_q\Omega_d\right) = 0,\\ &-\sum_{j=1}^{k}\mathcal{F}_{j+2,k+1}^{T}\nabla_{x_j}W + \mathcal{F}_{1,k+1}^{'T}\nabla_q\Omega_d = 0,\end{aligned} \quad (21)$$

which, computed at $(q,p) = (q^*,0)$, define the values $x_j^*$ for all $j \ge 1$ at the equilibrium, concluding the proof.□

*4.2. Second controller design*

The analytical expression of the control law (12) grows in size and complexity with $s$, thus potentially resulting in increasing computational load. In an attempt to mitigate this shortcoming, the elements of $\mathcal{F}'$ on the diagonal that refer to the actuator states $x_j$, with $1 \le j \le s$, are defined instead as

$$\mathcal{F}'_{j+2,j+2} = -K_j + \left( \mathcal{F}'^T_{1,j+2} \nabla_q \zeta_j + \mathcal{F}'^T_{2,j+2} \nabla_p \zeta_j + \sum_{i=1}^{j-1} \mathcal{F}'^T_{i+2,j+2} \nabla_{x_i} \zeta_j \right) \left( \nabla_{x_j} \zeta_j \right)^{-1}. \tag{22}$$

The expression of $\zeta_k$ for $k > 1$ that ensures matching between (8) and (9) for the states $(x_2, \ldots, x_s)$ becomes then

$$\begin{aligned} \zeta_k = & -\mathcal{F}^T_{1,k+1} \nabla_q W - \mathcal{F}^T_{2,k+1} \nabla_p W - \sum_{j=1}^{k} \mathcal{F}^T_{j+2,k+1} \nabla_{x_j} W \\ & + \mathcal{F}'^T_{1,k+1} \left( \nabla_q H_d + \left( \sum_{i=1}^{k-2} (\nabla_q \zeta_i)^T \zeta_i \right) \right) \\ & + \mathcal{F}'^T_{2,k+1} \left( M_d^{-1} p + \left( \sum_{i=1}^{k-2} (\nabla_p \zeta_i)^T \zeta_i \right) \right) \\ & + \sum_{j=1}^{k-2} \mathcal{F}'^T_{j+2,k+1} \left( \sum_{i=1}^{k-2} (\nabla_{x_j} \zeta_i)^T \zeta_i \right) + K_{k-1} (\nabla_{x_{k-1}} \zeta_{k-1})^T \zeta_{k-1}. \end{aligned} \tag{23}$$

Note that, differently from (10), $\zeta_k$ in (23) only contains $\zeta_{k-1}$ in the last term, thus resulting in a shorter expression. Similarly, the control law (12) becomes

$$\begin{aligned} u = & G_0^{-1} \left( \mathcal{F}^T_{1,s+2} \nabla_q W + \mathcal{F}^T_{2,s+2} \nabla_p W + \sum_{j=1}^{s} \mathcal{F}^T_{j+2,s+2} \nabla_{x_j} W \right) \\ & + G_0^{-1} \left( -\mathcal{F}'^T_{1,s+2} \left( \nabla_q H_d + \sum_{i=1}^{s-1} (\nabla_q \zeta_i)^T \zeta_i \right) \right) \\ & - G_0^{-1} \left( \mathcal{F}'^T_{2,s+2} \left( \nabla_p H_d + \sum_{i=1}^{s-1} (\nabla_p \zeta_i)^T \zeta_i \right) \right) \\ & + G_0^{-1} \left( + \sum_{j=1}^{s-1} \mathcal{F}'^T_{j+2,s+2} \left( \sum_{i=1}^{s-1} (\nabla_{x_j} \zeta_i)^T \zeta_i \right) - K_s (\nabla_{x_s} \zeta_s)^T \zeta_s \right). \end{aligned} \tag{24}$$

**Proposition 3.** *Consider the system (8) with Assumptions 1 to 3, with the control law (24) and the parameters (23). Then the closed-loop system is given by (9) with the matrix $\mathcal{F}'$ defined in (11) where the diagonal terms are given by (22).*

**Proof.** Equating the first rows in (8) and (9) yields again (13), while equating the second rows yields (14). Equating the third rows in (8) and (9) and substituting $\mathcal{F}'_{3,j+2}$ with $j > 2$ from (11) yields (18). Computing $\mathcal{F}'_{33}$ from (22) as

$$\mathcal{F}'_{33} = -K_1 + \left( \mathcal{F}'^T_{13} \nabla_q \zeta_1 + \mathcal{F}'^T_{23} \nabla_p \zeta_1 \right) (\nabla_{x_1} \zeta_1)^{-1},$$

and substituting it in (18) yields

$$\begin{aligned} & -\mathcal{F}^T_{23} \nabla_p W + \mathcal{F}_{33} \nabla_{x_1} W + \mathcal{F}_{34} \nabla_{x_2} W + \mathcal{F}'^T_{13} (\nabla_q H_d) + \mathcal{F}'^T_{23} \left( M_d^{-1} p \right) \\ & + K_1 \left( (\nabla_{x_1} \zeta_1)^T \zeta_1 \right) = \\ & -\mathcal{F}'^T_{13} \left( (\nabla_q \zeta_2)^T \zeta_2 \right) - \mathcal{F}'^T_{23} \left( (\nabla_p \zeta_2)^T \zeta_2 \right) + \mathcal{F}'_{33} (\nabla_{x_1} \zeta_2)^T \zeta_2 \\ & + \mathcal{F}'_{34} (\nabla_{x_2} \zeta_2)^T \zeta_2. \end{aligned} \tag{25}$$

The terms to the left of the equal correspond to $\zeta_2$ in (23), and substituting $\mathcal{F}'_{34}$ from (11) verifies (25). This same procedure is then repeated for the remaining states. Equating the last rows in (8) and (9) yields again (19). Substituting $\mathcal{F}'_{s+2,s+2}$ from (22) and computing the control input yields then (24) concluding the proof.□

**Proposition 4.** *Consider system (8) with Assumptions 1 to 3, in closed-loop with the control law (24) and the parameters (23). Then the equilibrium $x = x^*$, with $q = q^*$ and $p = p^* = 0$, is asymptotically stable for some $K_j > 0$, provided that either $(G k_v G^T + \frac{1}{2}(D M^{-1} M_d) + \frac{1}{2}(D M^{-1} M_d)^T) > 0$ or that $D = 0$ and the output $y = G^T M_d^{-1} p$ is detectable.*

**Proof.** Expressing $\mathcal{F}'_{j+2,j+2}$ as the sum of a symmetric part $\Phi_j$ and an antisymmetric part $\Psi_j$, that is $-\mathcal{F}'_{j+2,j+2} = K_j + \Phi_j + \Psi_j$, where $\Phi_j = \frac{1}{2}(-\mathcal{F}'_{j+2,j+2} - K_j) + \frac{1}{2}(-\mathcal{F}'_{j+2,j+2} - K_j)^T$ and $\Psi_j = -\frac{1}{2}(\mathcal{F}'_{j+2,j+2}) + \frac{1}{2}(\mathcal{F}'_{j+2,j+2})^T$, and computing the time derivative of $W_d$ along the trajectories of the closed-loop system (9) yields

$$\begin{aligned} \dot{W}_d = & -\nabla_p W_d^T \left( G k_v G^T + \Phi_0 \right) \nabla_p W_d \\ & - \sum_{j=1}^{s} \left( \nabla_{x_j} W_d^T \left( K_j + \Phi_j \right) \nabla_{x_j} W_d \right). \end{aligned} \tag{26}$$

Thus $\dot{W}_d \le 0$ and all states are bounded provided that $(G k_v G^T + \Phi_0) > 0$ and that $K_j + \Phi_j > 0$, where $\Phi_0$ has been defined in Proposition 2 and it follows from (22) that

$$\begin{aligned} \Phi_j = & \frac{1}{2} \left( \mathcal{F}'^T_{1,j+2} \nabla_q \zeta_j + \mathcal{F}'^T_{2,j+2} \nabla_p \zeta_j + \sum_{i=1}^{j-1} \mathcal{F}'^T_{i+2,j+2} \nabla_{x_i} \zeta_j \right) \left( \nabla_{x_j} \zeta_j \right)^{-1} \\ & + \frac{1}{2} \left( \mathcal{F}'^T_{1,j+2} \nabla_q \zeta_j + \mathcal{F}'^T_{2,j+2} \nabla_p \zeta_j + \sum_{i=1}^{j-1} \mathcal{F}'^T_{i+2,j+2} \nabla_{x_i} \zeta_j \right)^T \left( \nabla_{x_j} \zeta_j \right)^{-T}. \end{aligned}$$

It follows from (23) and Assumption 2 that $\nabla_{x_j} \zeta_j \neq 0$, while $(\mathcal{F}'^T_{1,j+2} \nabla_q \zeta_j + \mathcal{F}'^T_{2,j+2} \nabla_p \zeta_j + \sum_{i=1}^{j-1} \mathcal{F}'^T_{i+2,j+2} \nabla_{x_i} \zeta_j)$ is a sum of bounded terms. Thus there exists a sufficiently large $K_j$ that verifies the inequality $K_j + \Phi_j > 0$. The proof is completed by employing the same arguments used in Proposition 2, thus confirming that the equilibrium is asymptotically stable. □

**Remark 3.** In principle, it is possible to combine the controller designs (12) and (24) thus resulting in an hybrid implementation. For instance, defining $\zeta_k$ as in (10), $\mathcal{F}'_{s+2,s+2}$ as in (22), and the remaining elements of $\mathcal{F}'$ as in (11), yields again (24). This is however a different control law, since $\zeta_k$ are given in (10) rather than in (23). The corresponding stability conditions are then a combination of those given in Propositions 2 and 4, that is $K_j > 0$ for $j < s$, and $K_s + \Phi_s > 0$. The potential benefit of such approach is to combine the stronger stability properties of controller (12) (i.e., the weaker requirements on the parameters $K_j$) with the simpler expression of the control law resulting from (24).

## 5. Potential energy shaping

In this section, a variation of the controller (12) is proposed for a narrower class of systems in order to investigate whether it is possible to set $\mathcal{F}'_{11} \neq 0$ and what this would imply in terms of stability of the equilibrium. To this end, a further assumption is introduced which restricts the following result to a narrower class of underactuated mechanical systems.

**Assumption 4.** The inertia matrix $M$ is constant and diagonal, while $G \in \mathbb{R}^{n \times 1}$ and $\nabla_q^2 \Omega_d > 0$ are both constant, $G G^T$ is diagonal (i.e., $G$ is a standard basis vector), and $G G^T \nabla_q^2 \Omega_d^{-1} \ge 0$. In addition $\nabla_{x_j} E_k = 0, \ \forall j \neq k$ and $D = 0$.

The control law is designed such that the closed-loop dynamics is given by (9) where $W_d = \Omega_d + \frac{1}{2}\sum_{k=0}^{s}\zeta_k^T\zeta_k$ is a positive definite storage function, with $\zeta_k$ defined as

$$\zeta_k = \begin{cases} M^{-1}p + \Theta\nabla_q\Omega_d, & k=0 \\ G^\dagger\big(-\nabla_q W + \mathcal{F}_{23}\nabla_{x_1}W + \mathcal{F}'_{12}\big(\nabla_q\Omega_d + (\nabla_q\zeta_0)^T\zeta_0\big) + Gk_vG^T(\nabla_p\zeta_0)^T\zeta_0\big), & k=1 \\ -\mathcal{F}^T_{2,k+1}\nabla_p W - \sum_{j=1}^{k}\mathcal{F}^T_{j+2,k+1}\nabla_{x_j}W + \mathcal{F}'^T_{1,k+1}\big(\nabla_q\Omega_d + \sum_{i=0}^{k-1}(\nabla_q\zeta_i)^T\zeta_i\big) & \\ +\mathcal{F}'^T_{2,k+1}\big(\sum_{i=0}^{k-1}(\nabla_p\zeta_i)^T\zeta_i\big) + \sum_{j=1}^{k-1}\mathcal{F}'^T_{j+2,k+1}\big(\sum_{i=1}^{k-1}(\nabla_{x_j}\zeta_i)^T\zeta_i\big), & k>1. \end{cases} \tag{27}$$

Thus $\nabla_q\zeta_0 = \Theta\nabla_q^2\Omega_d$ and $\nabla_p\zeta_0 = M^{-1}$ are constant, while $\nabla_{x_1}\zeta_0 = 0$. The elements of $\mathcal{F}'$ on or above the diagonal (i.e. $\mathcal{F}'_{kj}$ on row $k$ and column $j \geq k$), are defined as in (11) apart from the terms

$$\begin{aligned} &\mathcal{F}'_{11} = -\Theta,\ \ \Theta^2 = \big(k_m GG^T\nabla_q^2\Omega_d^{-1}\big),\ \ \mathcal{F}'_{12} = \big(I + \Theta^2\nabla_q^2\Omega_d\big)M, \\ &\mathcal{F}'_{22} = -Gk_vG^T, \\ &\mathcal{F}'_{1,j+2} = \left(\Theta\nabla_q\zeta_j - \mathcal{F}'_{12}\nabla_p\zeta_j - \sum_{i=1}^{j-1}\big(\mathcal{F}'_{1,i+2}\nabla_{x_i}\zeta_j\big)\right)\big(\nabla_{x_j}\zeta_j\big)^{-1}, \end{aligned} \tag{28}$$

where $\Theta^2 = \Theta\Theta$, the parameter $k_m > 0$ is constant, and the control input is given by (12).

**Proposition 5.** *Consider system (8) with Assumptions 1 to 4, with the control law (12), and with the parameters (27) and (28). Then the closed-loop system is given by (9) with the matrix $\mathcal{F}'$ is defined according to (11) and (28).*

**Proof.** Equating the first rows in (8) and (9) yields

$$\begin{aligned} M^{-1}p = &-\Theta\left(\nabla_q\Omega_d + \sum_{k=0}^{s}(\nabla_q\zeta_k)^T\zeta_k\right) + \mathcal{F}'_{12}\sum_{k=0}^{s}(\nabla_p\zeta_k)^T\zeta_k \\ &+ \sum_{j=1}^{s}\left(\mathcal{F}'_{1,j+2}\sum_{k=j}^{s}(\nabla_{x_j}\zeta_k)^T\zeta_k\right). \end{aligned} \tag{29}$$

Defining $\zeta_0$ as in (27) and $\mathcal{F}'_{1j}$ as in (28) verifies (29).

Equating the second rows in (8) and (9) yields

$$\begin{aligned} &-\nabla_q\Omega + \mathcal{F}_{23}\nabla_{x_1}W = \\ &-\mathcal{F}'^T_{12}\left(\nabla_q\Omega_d + \sum_{k=0}^{s}(\nabla_q\zeta_k)^T\zeta_k\right) + \mathcal{F}'_{22}\sum_{k=0}^{s}(\nabla_p\zeta_k)^T\zeta_k \\ &+ \sum_{j=1}^{s}\left(\mathcal{F}'_{2,j+2}\sum_{k=j}^{s}(\nabla_{x_j}\zeta_k)^T\zeta_k\right). \end{aligned} \tag{30}$$

Defining $\mathcal{F}'_{2,j+2}$ with $j > 1$ according to (11) and substituting it in (30) cancels $\zeta_j$ for all $j > 1$. Pre-multiplying both sides of (30) by $G^\otimes = (G^\perp G^{\perp T})^{-1}G^\perp$ gives the matching condition

$$\begin{aligned} &G^\otimes\big(-\nabla_q\Omega + \mathcal{F}'^T_{12}\nabla_q\Omega_d\big) = \\ &G^\otimes\big(-\mathcal{F}'^T_{12}(\nabla_q\zeta_1)^T\zeta_1 + \mathcal{F}'_{22}(\nabla_p\zeta_1)^T\zeta_1 + \mathcal{F}'_{23}(\nabla_{x_1}\zeta_1)^T\zeta_1\big), \end{aligned} \tag{31}$$

where the terms to the left of the equal correspond to the PDE (6). Note that (31) does not contain $\zeta_0$ since $\mathrm{rank}(\Theta^2) = \mathrm{rank}(GG^T)$ hence $G^\perp\Theta\nabla_q^2\Omega_d\zeta_0 = 0$. Pre-multiplying both sides of (30) by $G^\dagger$ yields

$$\begin{aligned} &G^\dagger\big(-\nabla_q\Omega + \mathcal{F}_{23}\nabla_{x_1}W + \mathcal{F}'^T_{12}\nabla_q\Omega_d + \mathcal{F}'^T_{12}(\nabla_q\zeta_0)^T\zeta_0 \\ &\quad - \mathcal{F}'_{22}(\nabla_p\zeta_0)^T\zeta_0\big) = \\ &G^\dagger\big(-\mathcal{F}'^T_{12}(\nabla_q\zeta_1)^T\zeta_1 + \mathcal{F}'_{22}(\nabla_p\zeta_1)^T\zeta_1 + \mathcal{F}'_{23}(\nabla_{x_1}\zeta_1)^T\zeta_1\big), \end{aligned} \tag{32}$$

where the first line corresponds to $\zeta_1$. Thus, defining $\mathcal{F}'_{23}$ according to (11) solves both (31) and (32). The rest of the proof follows closely that of Proposition 1, thus it is omitted for brevity. □

**Proposition 6.** *Consider system (8) with Assumptions 1 to 4, in closed-loop with the control law (12) and the parameters (27) and (28). Assume in addition that $\Omega_d$ is quadratic in $q$. Then the equilibrium $x = x^*$, with $q = q^*$ and $p = p^* = 0$ is stable and $G^Tq$ converges to $G^Tq^*$ asymptotically for all $K_j > 0, k_v > 0, k_m > 0$, provided that $\Theta + \Theta^T \geq 0$.*

**Proof.** Recall that $W_d = \Omega_d + \frac{1}{2}\sum_{k=0}^{s}\zeta_k^T\zeta_k$ is positive definite. Computing its time derivative along the trajectories of the closed-loop system (9) yields

$$\begin{aligned} \dot{W}_d = &-\frac{1}{2}\nabla_q W_d^T\big(\Theta + \Theta^T\big)\nabla_q W_d - \nabla_p W_d^T\big(Gk_vG^T\big)\nabla_p W_d \\ &- \sum_{j=1}^{s}\big(\nabla_{x_j}W_d^TK_j\nabla_{x_j}W_d\big), \end{aligned} \tag{33}$$

where $\nabla_q W_d = \nabla_q\Omega_d + (\Theta\nabla_q^2\Omega_d)^T\zeta_0 + \sum_{j=1}^{s}((\nabla_q\zeta_j)^T\zeta_j)$, $\nabla_p W_d = M^{-1}\zeta_0 + \sum_{j=1}^{s}((\nabla_p\zeta_j)^T\zeta_j)$, and $\nabla_{x_i}W_d = \sum_{j=i}^{s}((\nabla_{x_i}\zeta_j)^T\zeta_j)$. Employing the same argument used in Proposition 2, it follows from (33) that $\dot{W}_d \leq 0$ for all $k_v > 0, K_j > 0$ and $k_m > 0$, where $(\Theta + \Theta^T) \geq 0$ by hypothesis, thus $q, \zeta_j \in \mathcal{L}^\infty$ for all $j \geq 0$. It follows from (28) that $\Theta^2$ is the product of the rank-deficient positive semidefinite diagonal matrix $GG^T$ and of the full-rank positive definite symmetric matrix $\nabla_q^2\Omega_d^{-1}$, thus it has the same rank as $GG^T$. Consequently, $G^T\nabla_q W_d, G^T\nabla_p W_d, \nabla_{x_j}W_d \in \mathcal{L}^2$ and thus $G^T\nabla_q\Omega_d, G^T\zeta_0, \zeta_{j>0} \in \mathcal{L}^2$. Finally, it follows from (9) that $\dot{q}, \dot{p}, \dot{\zeta}_j \in \mathcal{L}^\infty$. Thus $\zeta_{j>0}$, $G^T\zeta_0$, and $G^T\nabla_q\Omega_d$ are bounded and converge to zero asymptotically. Since $\Omega_d$ has a unique minimizer in $q = q^*$ by design and is quadratic in $q$ while $G$ is constant, the fact that $G^T\nabla_q\Omega_d$ converges to zero implies that $G^Tq$ converges to $G^Tq^*$. Finally, substituting $p = 0$ and $\zeta_j = 0$ in (27) yields again (21) which defines the values $x_j^*$ at the equilibrium. □

**Remark 4.** Although the parameters (27) and (28) do not explicitly enforce kinetic energy shaping, $\mathcal{F}'_{12}$ can be interpreted as the product of inertia matrices, that is

$$\big(I + \Theta^2\nabla_q^2\Omega_d\big)M = M^{-1}M_d.$$

Pre-multiplying both sides of the above equation by $M$ and substituting $\Theta^2$ from (28) yields

$$M_d = M\big(I + k_mGG^T\big)M,$$

which is constant and symmetric since it is the product of diagonal matrices, thus the PDE (5) is solved by $J_2 = 0$. The ability to shape the kinetic energy is however limited compared to the standard IDA-PBC control (3), since the parameter $k_m$ only affects the actuated states. Note that the proposed potential shaping design is not feasible in the presence of physical damping, since then the matching Eq. (30) would not be verified. Note also that the detectability condition typically required for the output $y = G^TM_d^{-1}p$ [18] is not present in Proposition 6. However, since $\Theta$ is chosen to be rank deficient in order to preserve the PDE (6) (see Proposition 5), its effect on the Lyapunov derivative (33) is limited to the actuated states. As a result, only asymptotic convergence to the equilibrium $G^Tq = G^Tq^*$ is concluded in Proposition 6. If $k_m = 0$ then $M_d = M$

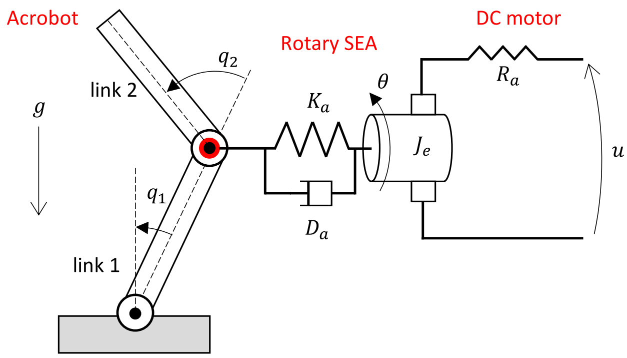


**Fig. 1.** Simplified schematic of the Acrobot system with a rotary SEA.

and $\Theta = 0$, thus stability of the equilibrium is only concluded if the output $y = G^T\zeta_0$ is detectable. Substituting $\zeta_0$ from (27) $k_m = 0$ yields $y = G^T M^{-1}p + G^T\Theta\nabla_q\Omega_d = G^T M^{-1}p$, thus recovering the detectablity condition in Ortega et al. [18]. In alternative to (28), it would be possible to define $\Theta^2 = k_m^2\, GG^T$ which is symmetric positive semidefinite and yields $\Theta = k_m GG^T \geq 0$. As a result, the condition $\Theta + \Theta^T \geq 0$ in Proposition 6 is automatically verified. However computing $M_d$ as above yields $M_d = M\left(I + k_m GG^T\nabla_q^2\Omega_d\right)M$ which is in general not symmetric and thus it does not represent the inertia matrix of any mechanical system.

## 6. Illustrative examples

The energy shaping controllers outlined in Sections 4 and 5 are demonstrated with three examples, namely an Acrobot system with a rotary series elastic actuator (SEA), a soft continuum manipulator actuated by electroactive polymers (EAP), and a two-mass-spring system actuated by a DC motor.

### *6.1. Acrobot system with SEA*

The Acrobot system [16] is modified by including a rotary series elastic actuator (SEA) consisting of a spring, a damper, and a DC motor, where the effect of the inductance is omitted for simplicity [4]. The Acrobot system consists of an articulated pendulum with a single actuator at the elbow joint $q_2$ and an unactuated shoulder joint $q_1$ (see Fig. 1). The open-loop dynamics of the mechanical sub-system is given by (1) with total energy $H = \Omega + \frac{1}{2}p^T M^{-1}p$ where $\Omega = g(c_4\cos(q_1) + c_5\cos(q_1+q_2))$, the input matrix is $G^T = \begin{bmatrix}0 & 1\end{bmatrix}$, while $M = \begin{bmatrix}c_1+c_2+2c_3\cos(q_2) & c_2+c_3\cos(q_2)\\ c_2+c_3\cos(q_2) & c_2\end{bmatrix}$ is the inertia matrix with determinant $\Delta = \det(M) > 0$. The terms $c_1, c_2, c_3, c_4, c_5$ are constant parameters depending on the size of the links, while $g$ is the gravity constant. The control goal is to stabilize the upright position $(q_1, q_2) = (0, 0)$, which is open-loop unstable. The IDA-PBC controller (3) for the Acrobot with direct actuation yields the control law [16]

$$u = \frac{1}{2}\nabla_{q_2}\left(p^T M^{-1}p\right) + \nabla_{q_2}\Omega$$
$$-\begin{bmatrix}k_2 & k_3\end{bmatrix}M^{-1}\nabla_q\Omega_d + \frac{k_v}{\Delta_d}(k_2p_1 - k_1p_2),$$

where $k_1, k_2, k_3, k_v$ are tuning parameters, $p = M\dot{q}$, while $\Omega_d$ and $\Delta_d$ are given in Appendix A. The complete system dynamics described with (8) yields

$$\mathcal{F}_{11} = \mathcal{F}_{13} = \mathcal{F}_{14} = \mathcal{F}_{24} = 0,\ \mathcal{F}_{12} = I,\ \mathcal{F}_{34} = \frac{1}{J_e},$$
$$\mathcal{R}_{22} = 0,\ \mathcal{F}_{23} = 0,\ \mathcal{R}_{33} = 0,\ \mathcal{R}_{44} = \frac{D_a}{J_e^2},\ G_0 = \frac{K_e}{R_aJ_e}$$

where $K_e$ and $R_a$ are the torque constant of the motor and the armature resistance respectively, while $D_a$ is the viscous friction of the SEA. The total energy of the system is $W = H + \frac{1}{2}K_a(q_2-\theta)^2 + \frac{1}{2}J_e\omega^2$, where $K_a$ is the stiffness of the SEA and $J_e$ is the moment of inertia of the motor. The system states are the position $q = (q_1, q_2)$, the momenta $p = M\dot{q}$, the angular position $x_1 = \theta$ of the SEA, and the angular velocity $x_2 = \omega = \dot{\theta}$ of the SEA. Note that $\mathcal{F}_{23} = 0$ but $\nabla_\theta\mathcal{F}_{12}^T\nabla_q W \neq 0$, thus Assumption 2 is verified. The energy of the mechanical sub-system in closed-loop is $H_d = \Omega_d + \frac{1}{2}p^T M_d^{-1}p$ as in D. Mahindrakar et al. [16], and the total energy of the complete system is $W_d = H_d + \frac{1}{2}\zeta_1^T\zeta_1 + \frac{1}{2}\zeta_2^T\zeta_2$, where it follows from (10) and (22) that

$$\zeta_1 = G^\dagger\left(-\nabla_q W + \mathcal{F}_{12}'\nabla_q H_d - \mathcal{F}_{22}'\nabla_p H_d\right),$$
$$\zeta_2 = \frac{1}{J_e}\nabla_\omega W + K_1(\nabla_\theta\zeta_1)^T\zeta_1 + \mathcal{F}_{23}'^T\nabla_p H_d + \mathcal{F}_{13}'^T\nabla_q H_d.$$

The elements of $\mathcal{F}'$ computed as in (11) and (22) are given in Appendix A. The control input computed as in (24) is

$$u = \left(K_e + \frac{R_aD_a}{K_e}\right)\omega + \frac{K_aR_a}{K_e}(\theta - q_2) - \frac{J_eR_a}{K_e}\mathcal{F}_{14}'^T\left(\nabla_q H_d + (\nabla_q\zeta_1)^T\zeta_1\right)$$
$$-\frac{J_eR_a}{K_e}\mathcal{F}_{24}'^T\left(\nabla_p H_d + (\nabla_p\zeta_1)^T\zeta_1\right) - \frac{J_eR_a}{K_e}\mathcal{F}_{34}'^T\left((\nabla_\theta\zeta_1)^T\zeta_1\right)$$
$$-K_2\frac{J_eR_a}{K_e}\left((\nabla_\omega\zeta_2)^T\zeta_2\right),$$

and it employs the parameters $\Omega_d, M_d$ and $J_2$, which are the solutions of the PDEs (5) and (6) for the Acrobot system with direct actuation [16].

Numerical simulations have been performed in Matlab using an ODE23 solver with the model parameters $c_1 = 0.23333$; $c_2 = 0.53333$; $c_3 = 0.2$; $c_4 = 0.3$; $c_5 = 0.2$; $g = 9.81$; $R_a = 0.5$; $K_e = 1$; $J_e = 10^{-3}$; $D_a = 1$; $K_a = 10$. The tuning parameters have been chosen empirically as $k_0 = -35$; $k_1 = 0.03386$; $k_2 = 0.1$; $k_3 = 0.59073$; $\mu = -0.6019$; $k_u = 1$; $k_v = 2$; $K_1 = 10^3$; $K_2 = 10^4$. The system response with the controller (24) is shown in Fig. 2: the position reaches the prescribed equilibrium $(q_1, q_2) = (0, 0)$ in a similar fashion to the mechanical system with direct actuation and the IDA-PBC controller (3) (see Fig. 2(a) and (g)). The angular position $\theta$ and the angular velocity $\omega = \dot{\theta}$ of the motor are shown in Fig. 2(d) and (e) (no gearbox has been included in the model for simplicity). The control input computed as in (24) corresponds to a voltage (see Fig. 2(c)) thus it is not directly comparable with controller (3). Instead, the motor torque has the same order of magnitude with both controllers (see Fig. 2(f) and (i)).

### *6.2. Soft continuum manipulator with EAP actuation*

The dynamics of a soft continuum manipulator of mass $m$ and length $l$ moving on the horizontal plane and actuated by electroactive polymers (EAP) [15] described with (8) yields the parameters

$$\mathcal{F}_{11} = \mathcal{F}_{13} = \mathcal{F}_{14} = \mathcal{F}_{24} = 0,\ \mathcal{F}_{12} = \mathcal{F}_{34} = I,\ \mathcal{R}_{22} = D,$$
$$\mathcal{F}_{23} = K_cG,\ \mathcal{R}_{33} = R_2,\ \mathcal{R}_{44} = R_1,\ G_0 = I,$$

where $R_1, R_2$ are resistances, and $K_c$ represents the coupling between EAP and soft continuum manipulator. The latter is modeled as a rigid-link system with $n = 2$ virtual elastic joints of stiffness $k$ and damping $D$ [27], where only the first is actuated thus $G^T = \begin{bmatrix}1 & 0\end{bmatrix}$ (see Fig. 3). The total energy of the mechanical sub-system is $H = \Omega + \frac{1}{2}p^T M^{-1}p$, where $\Omega = \frac{1}{2}k(q_1^2 + q_2^2)$ with $q_1$ and $q_2$ the angles of the virtual joints, and $M = \frac{ml^2}{4}\begin{bmatrix}4\cos(q_2)+6 & 2\cos(q_2)+1\\ 2\cos(q_2)+1 & 1\end{bmatrix}$. The total energy of the complete system is $W = H + \frac{1}{2C}Q^2 + \frac{1}{2L}\phi^2$, where $C$ is the capacitance

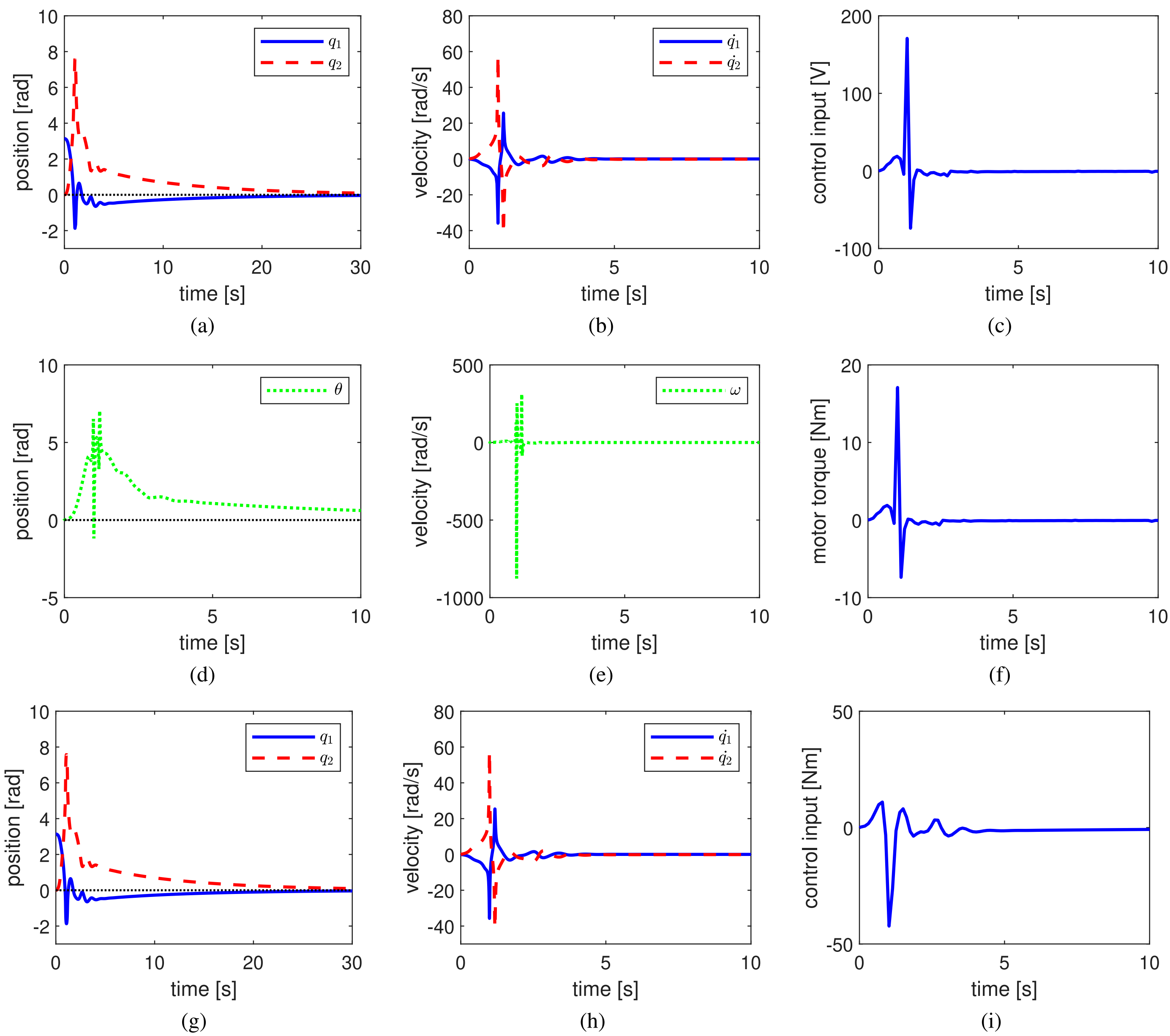


**Fig. 2.** Simulation results for the Acrobot with either a SEA or with direct actuation: (a) position with SEA and controller (24); (b) velocity; (c) control input with (24); (d) motor position $\theta$; (e) motor velocity $\omega$; (f) motor torque with (24); (g) position with direct actuation and with controller (3); (h) velocity; (i) control input with (3).

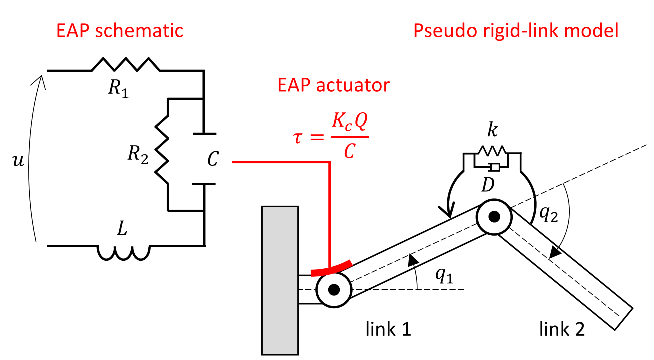


**Fig. 3.** Simplified schematic of the soft continuum manipulator with EAP actuation.

and $L$ is the inductance of the EAP. The system states are the position $q=(q_1,q_2)$, the momenta $p=M\dot{q}$, the electric charge $x_1 = Q$, and the flux $x_2=\phi$. The control goal is to stabilize the position $(q_1,q_2)=(q_1^*,0)$ where, differently from the Acrobot, $q_2=0$ is open-loop stable.

The energy of the mechanical sub-system in closed-loop is $H_d=\Omega_d+\frac{1}{2}p^T M_d^{-1}p$, where $M_d=k_m M$ and $\Omega_d=\frac{1}{2}\left(k_p(q_1-q_1^*)^2+\frac{k}{k_m}q_2^2\right)$ with $k_p$ and $k_m$ tuning parameters, and the control law computed as in (3) is

$$u = kq_1 + k_p k_m(q_1^*-q_1) - \frac{4k_v(p_2-p_1+2p_2\cos(q_2))}{ml^2\left(4\cos(q_2)^2-5\right)}.$$

Note that setting $M_d=k_m M$ solves the PDE (5) with $J_2=0$. The total energy of the complete system in closed loop is $W_d=H_d+\frac{1}{2}\zeta_1^T\zeta_1+\frac{1}{2}\zeta_2^T\zeta_2$, where it follows from (10) that

$$\begin{aligned}\zeta_1 &= G^\dagger\left(-\nabla_q H + K_c G\nabla_Q W + \mathcal{F}_{12}'\nabla_q H_d + Gk_v G^T\nabla_p H_d\right),\\ \zeta_2 &= -K_c G^T\nabla_p H - R_2\nabla_Q W + \nabla_\phi W - \mathcal{F}_{33}'(\nabla_Q\zeta_1)^T\zeta_1\\ &\quad + \mathcal{F}_{23}'^T\left(\nabla_p H_d + (\nabla_p\zeta_1)^T\zeta_1\right) + \mathcal{F}_{13}'^T\left(\nabla_q H_d + (\nabla_q\zeta_1)^T\zeta_1\right).\end{aligned}$$

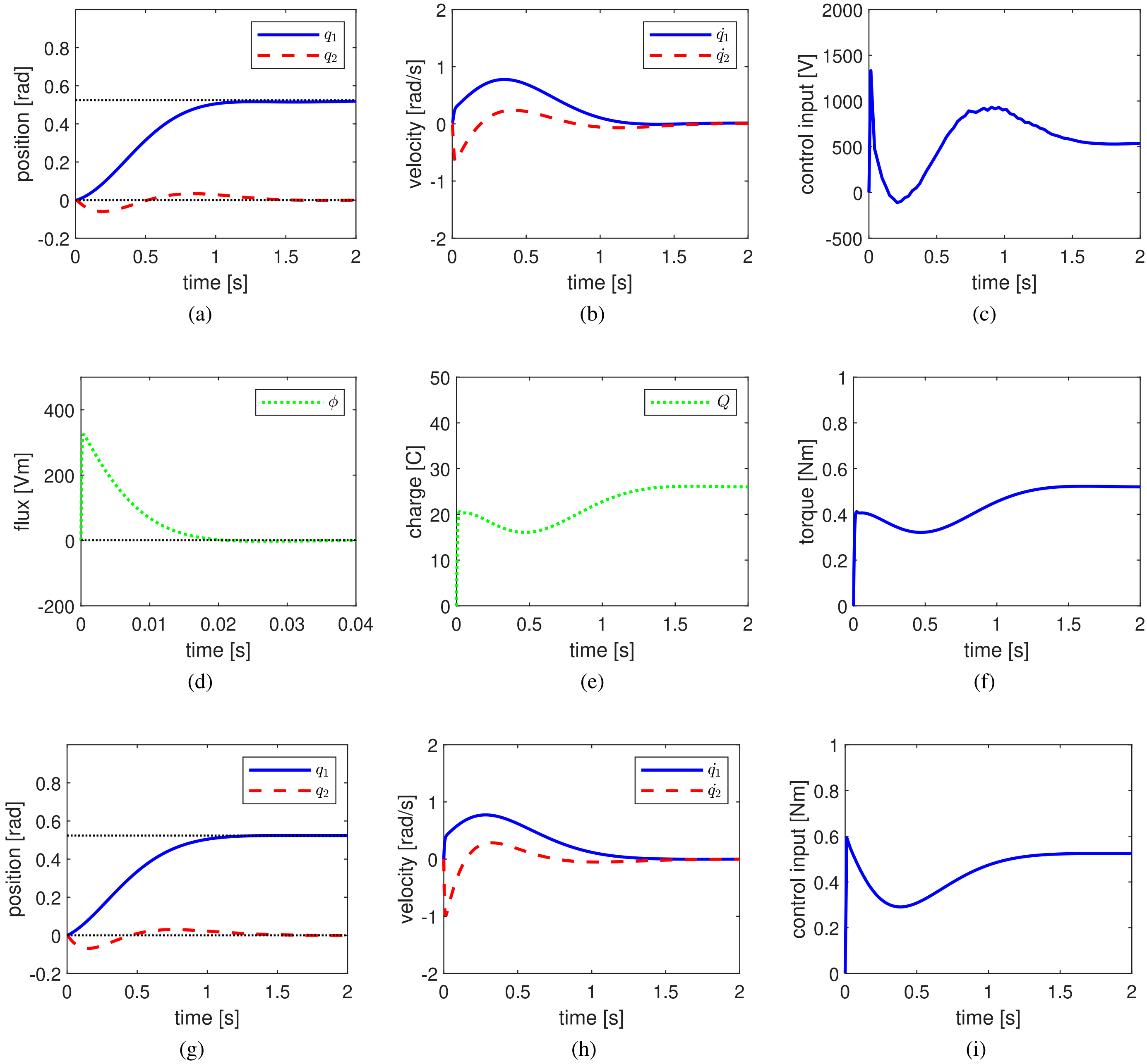


**Fig. 4.** Simulation results for soft continuum manipulator with either EAP actuation or with direct actuation: (a) position with EAP and controller (24); (b) velocity; (c) control input with (24); (d) flux $\phi$; (e) charge Q; (f) torque with (24); (g) position with direct actuation and with controller (3); (h) velocity; (i) control input with (3).

The elements of $\mathcal{F}'$ computed as in (11) are given in Appendix B. For comparison purposes, $\zeta_1$ and $\zeta_2$ computed as in (23) are given by

$$\begin{aligned}\zeta_1 &= G^{\dagger}\big(-\nabla_q H + K_c G \nabla_Q W + \mathcal{F}'^{T}_{12}\nabla_q H_d + G k_v G^T \nabla_p H_d\big),\\ \zeta_2 &= -K_c G^T \nabla_p H - R_2 \nabla_Q W + \nabla_\phi W + K_1 (\nabla_Q \zeta_1)^T \zeta_1\\ &\quad + \mathcal{F}'^{T}_{23}(\nabla_p H_d) + \mathcal{F}'^{T}_{13}(\nabla_q H_d).\end{aligned}$$

Finally, the controller (24) yields

$$\begin{aligned}u = \frac{Q}{C} + R_1\frac{\phi}{L} &- \mathcal{F}'^{T}_{14}\big(\nabla_q H_d + (\nabla_q \zeta_1)^T \zeta_1\big)\\ &- \mathcal{F}'^{T}_{24}\big(\nabla_p H_d + (\nabla_p \zeta_1)^T \zeta_1\big) - \mathcal{F}'^{T}_{34}\big((\nabla_Q \zeta_1)^T \zeta_1\big)\\ &- K_2\big((\nabla_\phi \zeta_2)^T \zeta_2\big).\end{aligned}$$

Numerical simulations have been performed in Matlab using an ODE23 solver with the model parameters $m = 1.5$; $l = 0.15$; $k = 1$; $D = 0.15$; $R_1 = 30$; $R_2 = 1.4 \times 10^{-3}$; $K_c = 10^{-3}$; $C = 0.05$; $L = 0.1$. The tuning parameters for the IDA-PBC controller (3) have been chosen empirically as $k_p = 0.75$, $k_m = 2$, and $k_v = 0.5$. The tuning parameters for the controller (24) have been chosen as $k_p = 0.75$, $k_m = 2$, $k_v = 0.5$, $K_1 = 1$ and $K_2 = 120$ for consistency. The system response with the controller (3) for the mechanical sub-system and with the controller (24) for the complete system is shown in Fig. 4: the position reaches the prescribed equilibrium $(q_1, q_2) = (\pi/6, 0)$ with a similar transient for both controllers applied to the corresponding systems (see Fig. 4(a) and (g)). The flux $\phi$ and the charge $Q$ corresponding to the EAP are shown in Fig. 4(d) and (e). The control input computed as in (24) corresponds to a voltage (see Fig. 4(c)) and its magnitude (i.e., kV range)

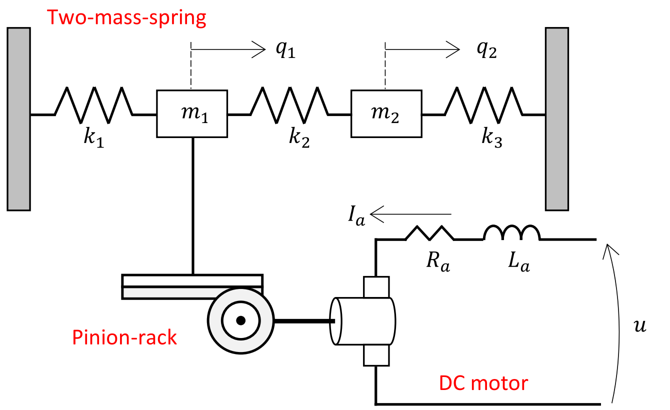


**Fig. 5.** Simplified schematic of the two-mass-spring system actuated by a DC motor.

is representative of EAP actuators [25]. The resulting torque has the same order of magnitude as the control input computed with (3) for the mechanical sub-system (see Fig. 4(f) and (i)). Note that employing the controller (3), which does not account for EAP actuation, on the complete system (8) yields $q_1 \approx q_2 \approx 0$, thus the regulation goal $(q_1, q_2) = (\pi/6, 0)$ is not achieved (see Appendix B). The hybrid implementation discussed in Remark 3 with the same tuning parameters yields similar results, which have been included in Appendix B for completeness.

### 6.3. Two-mass-spring system with DC motor

The two-mass-spring system presented in Bastos and Franco [1] is modified here by introducing a DC motor for the actuation, and by removing the damper in order to comply with Assumption 4. The positions of the masses are $q_1$ and $q_2$, and the springs have stiffness $k_1$, $k_2$, and $k_3$ (see Fig. 5). The energy

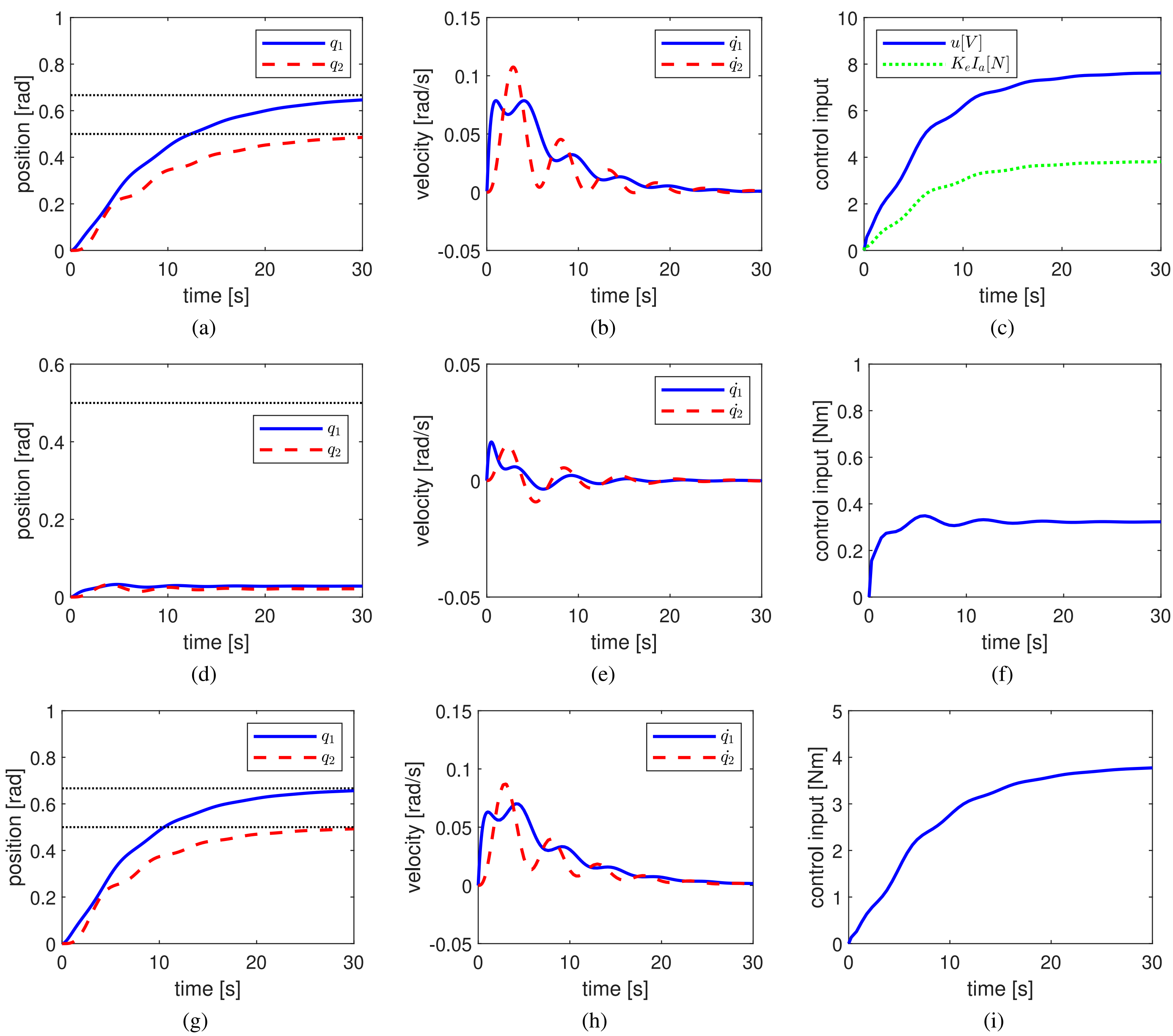


**Fig. 6.** Simulation results for the two-mass-spring system with either DC motor actuation or with direct actuation: (a) position with DC motor and with controller (12); (b) velocity; (c) control input and corresponding torque with (12); (d) position with DC motor and with controller (3); (e) velocity; (f) control input with (3); (g) position with direct actuation and with controller (3); (h) velocity; (i) control input with (3).

of the mechanical sub-system is $H = \Omega + \frac{1}{2}m_1\dot{q}_1^2 + \frac{1}{2}m_2\dot{q}_2^2$, where $\Omega = \frac{k_1 q_1^2}{2} + \frac{k_2(q_2-q_1)^2}{2} + \frac{k_3 q_2^2}{2}$, the inertia matrix is $M = \begin{bmatrix} m_1 & 0 \\ 0 & m_2 \end{bmatrix}$, and the input matrix is $G^T = \begin{bmatrix} 1 & 0 \end{bmatrix}$. The control goal corresponds to moving the second mass to a prescribed position such that $(q_1, q_2) = (q_1^*, q_2^*)$, where $q_1^*$ depends on $q_2^*$, that is $q_1^* = q_2^* \frac{k_2+k_3}{k_2}$, since the system is underactuated.

Employing the IDA-PBC design (3) yields the control law

$$u = k_1 q_1 \ + k_2(q_1 - q_2) + \frac{a_1 m_2\left(k_2 q_2 - k_2 q_1 + k_3 q_2^*\right)}{a_3 m_1} - \frac{k_v m_1 \dot{q}_1}{a_1},$$

where $k_v, a_1, a_3$ are tuning parameters, the closed-loop system has constant inertia matrix $M_d = \begin{bmatrix} a_1 & 0 \\ 0 & a_3 \end{bmatrix}$, and the potential energy is

$$\Omega_d = \left(\frac{k_2}{2}\left(q_1 + q_2^* - q_2^*\frac{(k_2+k_3)}{k_2}\right)^2 + \frac{1}{2}q_2^2(k_2+k_3) - k_2 q_1 q_2\right)\frac{m_2}{a_3} + \frac{k_3 m_2 q_2^{*^2}}{2a_3}.$$

Accounting for the dynamics of a DC motor with negligible inertia that actuates the first mass through a pinion-rack arrangement, the total energy of the system becomes $W = H + \frac{1}{2}L_a I_a^2$, where $L_a$ is the inductance of the motor and $I_a$ is the armature current. The complete system dynamics described with (8) yields

$$\mathcal{F}_{11} = \mathcal{F}_{13} = 0,\ \mathcal{F}_{12} = I,\ \mathcal{R}_{22} = 0,\ \mathcal{F}_{23} = G\frac{K_e}{L_a},\ \mathcal{R}_{33} = \frac{R_a}{L_a^2},\ G_0 = \frac{1}{L_a},$$

where $K_e$ and $R_a$ are the torque constant of the motor and the armature resistance respectively. The system states are the position $q = (q_1, q_2)$, the momenta $p = M\dot{q}$, and the armature current $x_1 = I_a$. The total energy of the closed-loop system is $W_d = \Omega_d + \frac{1}{2}\zeta_0^T\zeta_0 + \frac{1}{2}\zeta_1^T\zeta_1$, where it follows from (27) that

$$\begin{aligned} \zeta_0 &= M^{-1}p + \Theta\nabla_q\Omega_d, \\ \zeta_1 &= G^\dagger\left(-\nabla_q\Omega + \mathcal{F}_{12}'\left(\nabla_q\Omega_d + (\nabla_q\zeta_0)^T\zeta_0\right)\right) \\ &\quad + G^\dagger\left(+\frac{K_e}{L_a}G\nabla_I W + Gk_v G^T\left((\nabla_p\zeta_0)^T\zeta_0\right)\right). \end{aligned}$$

The elements of $\mathcal{F}'$ computed as in (11) and (28) are given in Appendix C. The controller (12) that achieves potential energy shaping according to Proposition 5 (see Section 5) is

$$\begin{aligned} u &= K_e\dot{q}_1 + R_a I_a - L_a\mathcal{F}_{13}'^T\left(\nabla_q H_d + (\nabla_q\zeta_0)^T\zeta_0 + (\nabla_q\zeta_1)^T\zeta_1\right) \\ &\quad - L_a\mathcal{F}_{23}'^T\left(\nabla_p H_d + (\nabla_p\zeta_0)^T\zeta_0 + (\nabla_p\zeta_1)^T\zeta_1\right) - K_1 L_a\left((\nabla_{I_a}\zeta_1)^T\zeta_1\right), \end{aligned}$$

where the potential energy $\Omega_d$ is given above with $a_3 = m_2^2$ and $a_1 = (1+k_m)m_1^2$, and $k_m$ is a tuning parameter.

Numerical simulations have been performed in Matlab using an ODE23 solver with the model parameters $m_1 = 1;\ m_2 = 3;\ k_1 = 5;\ k_2 = 3; k_3 = 1;\ R_a = 10;\ K_e = 5;\ L_a = 10^{-2}$. The tuning parameters for the controller (12) corresponding to the complete system have been chosen empirically as $k_m = 0.01$ and $k_v = 2$, while the parameters for the controller (3) corresponding to the mechanical sub-system have been set to $a_1 = (1+k_m)m_1^2 = 1.01, a_3 = m_2^2 = 9$, and $k_v = 2$ for consistency. The system response with both controllers for the corresponding models is shown in Fig. 6: employing the controller (12) for the complete system the position reaches the prescribed equilibrium $(q_1, q_2) = (0.5, 0.67)$ in a smooth fashion (see Fig. 6(a)), and the transient response is similar to that of the mechanical sub-system with the IDA-PBC controller (3) (see Fig. 6(g)). Conversely, employing the controller (3) for the complete system (8) results in a large steady-state error (see Fig. 6(d)), since in this case the actuator dynamics is not accounted for in the controller design. Comparing Fig. 6(c) and (i) shows that the force produced by the motor is comparable to the control input computed as in (3) for the system with direct actuation.

## 7. Conclusion

This paper has presented some new results on the energy shaping control for a class of underactuated mechanical systems with high-order actuator dynamics. A controller design procedure which preserves the port-Hamiltonian structure of the closed-loop system and builds upon the IDA-PBC methodology in a modular fashion has been outlined. Two alternative controllers that achieve potential and kinetic energy shaping as well as damping assignment have been detailed. In addition, a variation of the controller design has been discussed for a narrower class of systems, which is characterized by constant and diagonal inertia matrix, resulting in different stability conditions.

The simulation results demonstrate that the proposed controllers effectively achieve the prescribed regulation goal for three different underactuated mechanical systems with corresponding actuator dynamics. In addition, the controllers employ the same potential and kinetic energy shaping and damping assignment as the traditional IDA-PBC for mechanical systems with direct actuation, thus resulting in a similar transient. Conversely, employing the traditional IDA-PBC controller alone, which neglects the actuator dynamics, can result in degraded performance. Future work will aim to relax the initial assumptions and to extend the results to multiple interconnected underactuated mechanical systems.

## Declaration of Competing Interest

The authors declare that they have no known competing financial interests or personal relationships that could have appeared to influence the work reported in this paper.

## CRediT authorship contribution statement

**Enrico Franco:** Conceptualization, Formal analysis, Investigation, Software, Visualization, Writing – original draft. **Alessandro Astolfi:** Conceptualization, Formal analysis, Investigation, Writing – review & editing.

## Acknowledgement

This research was supported by the Engineering and Physical Sciences Research Council (grant agreement nos. EP/W004224/1, EP/R511547/1, and EP/W005557/1), the European Union's Horizon 2020 Research and Innovation Programme under grant agreement no. 739551 (KIOS CoE), and the Italian Ministry for Research (2017 Program for Research Projects of National Interest under Grant 2017YKXYXJ, and 2020 Program for Research Projects of National Interest under Grant 2020RTWES4).

## Appendix A

Design parameters of the Acrobot system with direct actuation.

$$\begin{aligned} \nabla_{q_1}\Omega_d &= -k_0\sin(q_1 - \mu q_2) - b_1\sin(q_1) - b_2\sin(q_1+q_2) \\ &\quad - b_3\sin(q_1+2q_2) - b_4\sin(q_1-q_2) + k_u(q_1 - \mu q_2), \\ \nabla_{q_2}\Omega_d &= k_0\mu\sin(q_1 - \mu q_2) - b_2\sin(q_1+q_2) \\ &\quad -2b_3\sin(q_1+2q_2) + b_4\sin(q_1-q_2) - k_u(q_1 - \mu q_2), \\ M_d &= \begin{bmatrix} k_1 & k_2 \\ k_2 & k_3 \end{bmatrix},\ b_1 = \frac{g}{2k_2}\left(c_3c_4 \pm 2c_4\sqrt{c_1c_2}\right), \end{aligned}$$

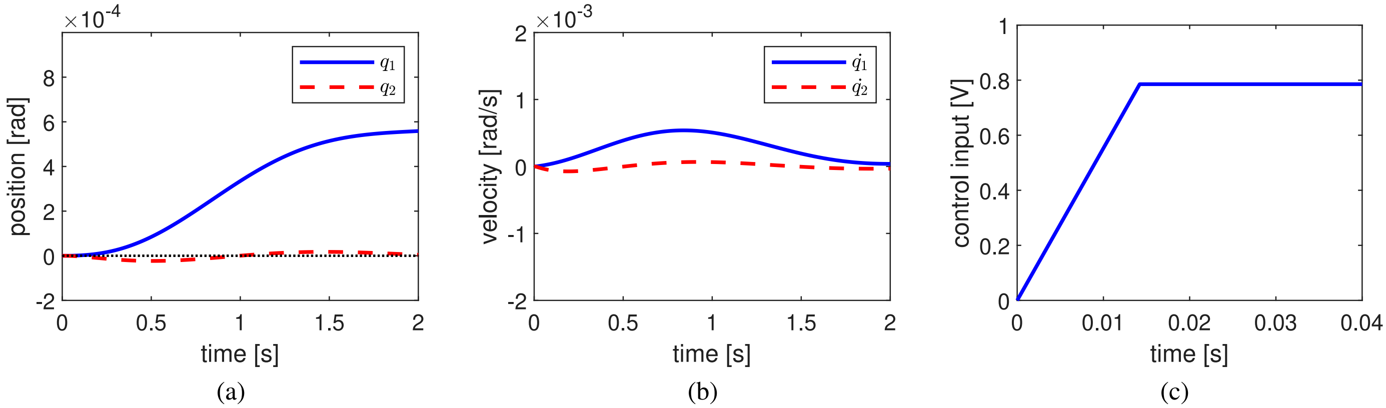


**Fig. B1.** Simulation results for soft continuum manipulator with EAP actuation using the IDA-PBC controller defined as in (3): (a) position; (b) velocity; (c) control input in [V].

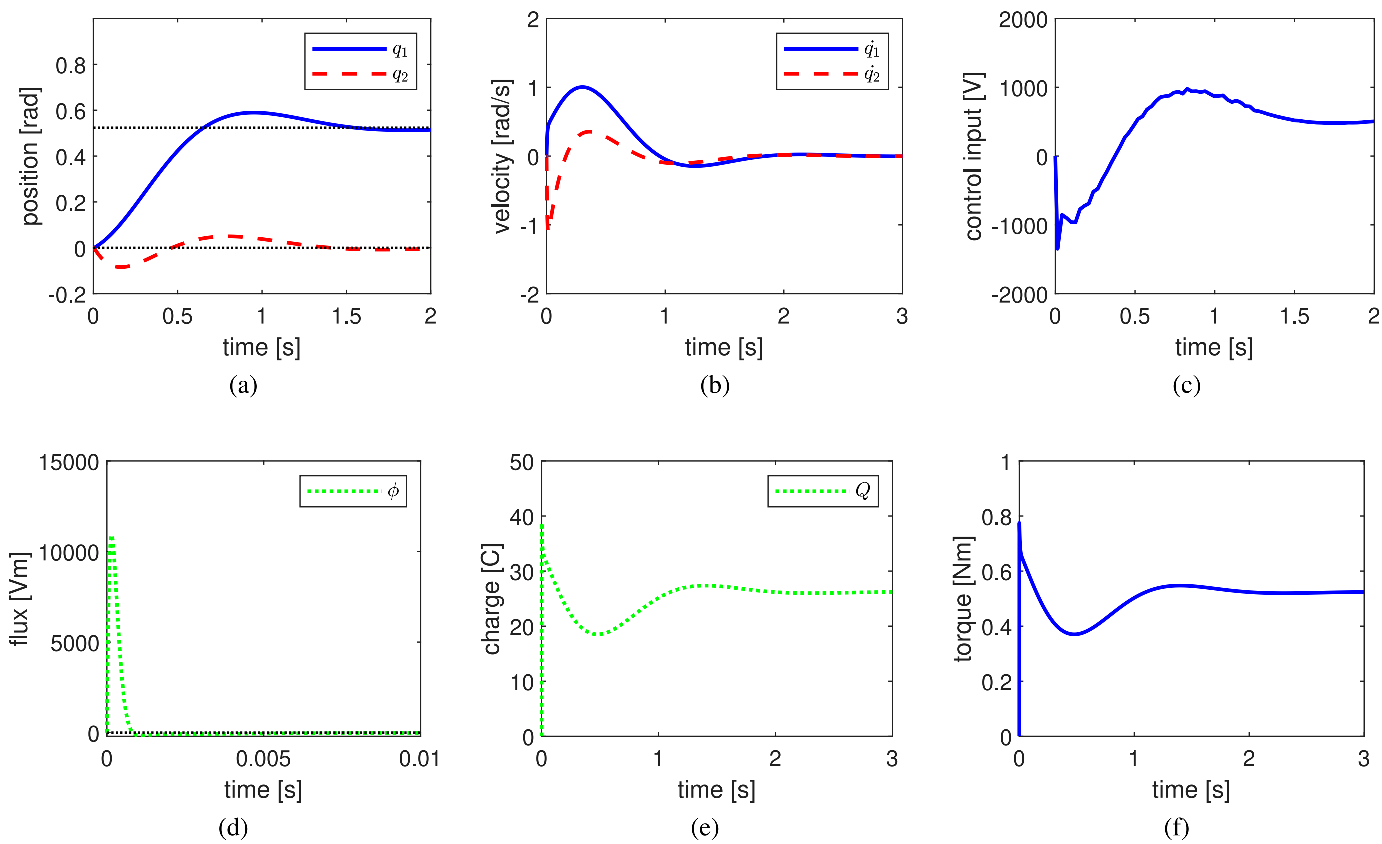


**Fig. B2.** Simulation results for soft continuum manipulator with EAP actuation using the hybrid implementation discussed in *Remark 3*: (a) position; (b) velocity; (c) control input; (d) flux $\phi$; (e) charge $Q$; (f) torque.

$$b_2 = \frac{g\mu}{2k_2(\mu+1)}\left(c_3c_4 \pm 2c_5\sqrt{c_1c_2}\right),$$

$$b_3 = \frac{g\mu c_3c_5}{2k_2(\mu+2)},\ \ b_4 = \frac{g\mu c_3c_4}{2k_2(\mu-1)},\ \ \Delta_d = k_1k_3 - k_2^2.$$

Elements of $\mathcal{F}'$ computed as in (11) and (22) for the Acrobot system with rotary SEA.

$$\mathcal{F}'_{12} = M^{-1}M_d,\ \ \mathcal{F}'_{13} = -\left(\mathcal{F}'_{12}\nabla_p\zeta_1\right)(\nabla_\theta\zeta_1)^{-1},$$

$$\mathcal{F}'_{14} = -\left(\mathcal{F}'_{12}\nabla_p\zeta_2 + \mathcal{F}'_{13}\nabla_\theta\zeta_2\right)(\nabla_\omega\zeta_2)^{-1},\ \ \mathcal{F}'_{22} = -Gk_vG^T,$$

$$\mathcal{F}'_{23} = G\left(1 + G^\dagger\mathcal{F}'^T_{12}\nabla_q\zeta_1 - G^\dagger\mathcal{F}'_{22}\nabla_p\zeta_1\right)(\nabla_\theta\zeta_1)^{-1} + G^{\perp T}\left(G^\otimes\mathcal{F}'^T_{12}\nabla_q\zeta_1 - G^\otimes\mathcal{F}'_{22}\nabla_p\zeta_1\right)(\nabla_\theta\zeta_1)^{-1},$$

$$\mathcal{F}'_{24} = \left(\mathcal{F}'^T_{12}\nabla_q\zeta_2 - \mathcal{F}'_{22}\nabla_p\zeta_2 - \mathcal{F}'_{23}\nabla_\theta\zeta_2\right)(\nabla_\omega\zeta_2)^{-1},$$

$$\mathcal{F}'_{34} = \left(1 + \mathcal{F}'^T_{13}\nabla_q\zeta_2 + \mathcal{F}'^T_{23}\nabla_p\zeta_2 - \mathcal{F}'_{33}\nabla_\theta\zeta_2\right)(\nabla_\omega\zeta_2)^{-1},$$

$$\mathcal{F}'_{33} = -K_1 + \left(\mathcal{F}'^T_{13}\nabla_q\zeta_1 + \mathcal{F}'^T_{23}\nabla_p\zeta_1\right)(\nabla_\theta\zeta_1)^{-1},$$

$$\mathcal{F}'_{44} = -K_2 + \left(\mathcal{F}'^T_{14}\nabla_q\zeta_2 + \mathcal{F}'^T_{24}\nabla_p\zeta_2 + \mathcal{F}'^T_{34}\nabla_\theta\zeta_2\right)(\nabla_\omega\zeta_2)^{-1}.$$

## Appendix B

Elements of $\mathcal{F}'$ computed as in (11) for the soft continuum manipulator with EAP actuation.

$$\mathcal{F}'_{22} = -k_mD - Gk_vG^T,\ \ \mathcal{F}'_{13} = -\left(\mathcal{F}'_{12}\nabla_p\zeta_1\right)(\nabla_Q\zeta_1)^{-1},$$

$$\mathcal{F}'_{14} = -\left(\mathcal{F}'_{12}\nabla_p\zeta_2 + \mathcal{F}'_{13}\nabla_Q\zeta_2\right)\left(\nabla_\phi\zeta_2\right)^{-1},\ \ \mathcal{F}'_{33} = -K_1,$$

$$\mathcal{F}'_{44} = -K_2,\ \mathcal{F}'_{23} = G\left(1 + G^{\dagger}\mathcal{F}'^{T}_{12}\nabla_q\zeta_1 - G^{\dagger}\mathcal{F}'_{22}\nabla_p\zeta_1\right)(\nabla_Q\zeta_1)^{-1}$$
$$+ G^{\perp T}\left(G^{\otimes}\mathcal{F}'^{T}_{12}\nabla_q\zeta_1 - G^{\otimes}\mathcal{F}'_{22}\nabla_p\zeta_1\right)(\nabla_Q\zeta_1)^{-1},$$
$$\mathcal{F}'_{24} = \left(\mathcal{F}'^{T}_{12}\nabla_q\zeta_2 - \mathcal{F}'_{22}\nabla_p\zeta_2 - \mathcal{F}'_{23}\nabla_Q\zeta_2\right)\left(\nabla_\phi\zeta_2\right)^{-1},$$
$$\mathcal{F}'_{34} = \left(1 + \mathcal{F}'^{T}_{13}\nabla_q\zeta_2 + \mathcal{F}'^{T}_{23}\nabla_p\zeta_2 - \mathcal{F}'_{33}\nabla_Q\zeta_2\right)\left(\nabla_\phi\zeta_2\right)^{-1}.$$

Elements on the diagonal of $\mathcal{F}'$ defined as in (22).

$$\mathcal{F}'_{33} = -K_1 + \left(\mathcal{F}'^{T}_{13}\nabla_q\zeta_1 + \mathcal{F}'^{T}_{23}\nabla_p\zeta_1\right)(\nabla_Q\zeta_1)^{-1},$$
$$\mathcal{F}'_{44} = -K_2 + \left(\mathcal{F}'^{T}_{14}\nabla_q\zeta_2 + \mathcal{F}'^{T}_{24}\nabla_p\zeta_2 + \mathcal{F}'^{T}_{34}\nabla_Q\zeta_2\right)\left(\nabla_\phi\zeta_2\right)^{-1}.$$

Simulation results for the soft continuum manipulator with EAP actuation using the IDA-PBC controller (3) are shown in Fig. B1. Note that the position does not reach the prescribed value $(q_1, q_2) = (\pi/6, 0)$ since the control input (i.e., in Volt) is insufficient to activate the EAP.

Simulation results for the soft continuum manipulator with EAP actuation using the hybrid implementation discussed in *Remark 3* are shown in Fig. B2: $\zeta_1, \zeta_2$ are defined as in (10), $\mathcal{F}'_{44}$ as in (22), and the remaining elements of $\mathcal{F}'$ as in (11). For consistency, the tuning parameters are the same as those employed in Section 6.2.

## Appendix C

Elements of $\mathcal{F}'$ computed as in (11) and (28) for the two-mass-spring system with DC motor actuation.

$$\Theta^2 = k_m G G^T(\nabla_q^2\Omega_d),\ \mathcal{F}'_{12} = \left(I + k_m G G^T\right)M,\ \mathcal{F}'_{22} = -G k_v G^T,$$
$$\mathcal{F}'_{13} = \left(-\mathcal{F}'_{12}\nabla_p\zeta_1 + \mathcal{F}'_{11}\nabla_q\zeta_1\right)(\nabla_{I_a}\zeta_1)^{-1},$$
$$\mathcal{F}'_{23} = G\left(1 + G^{\dagger}\mathcal{F}'^{T}_{12}\nabla_q\zeta_1 - G^{\dagger}\mathcal{F}'_{22}\nabla_p\zeta_1\right)(\nabla_{I_a}\zeta_1)^{-1}$$
$$+ G^{\perp T}\left(G^{\otimes}\mathcal{F}'^{T}_{12}\nabla_q\zeta_1 - G^{\otimes}\mathcal{F}'_{22}\nabla_p\zeta_1\right)(\nabla_{I_a}\zeta_1)^{-1},\ \mathcal{F}'_{33} = -K_1.$$

## References


[1] G. Bastos, E. Franco, Energy shaping dynamic tube-MPC for underactuated mechanical systems, Nonlinear Dyn. 106 (2021) 359–380, doi:10.1007/s11071-021-06863-9.

[2] G. Chen, W. Huo, Angular velocity stabilization of underactuated rigid satellites based on energy shaping, J. Frankl. Inst. 359 (4) (2022) 1558–1581, doi:10.1016/j.jfranklin.2022.01.001.

[3] A. Donaire, J.G. Romero, R. Ortega, B. Siciliano, Robust IDA-PBC for underactuated mechanical systems subject to matched disturbances, Int. J. Robust Nonlinear Control 27 (6) (2017) 1000–1016, doi:10.1002/rnc.3615.

[4] M.J. Fotuhi, Z. Ben Hazem, Z. Bingul, Modelling and torque control of an nonlinear friction inverted pendulum driven with a rotary series elastic actuator, in: 3rd International Symposium on Multidisciplinary Studies and Innovative Technologies, ISMSIT 2019 - Proceedings, Institute of Electrical and Electronics Engineers Inc., 2019, pp. 1–6, doi:10.1109/ISMSIT.2019.8932720.

[5] E. Franco, A. Astolfi, Energy shaping control of underactuated mechanical systems with fluidic actuation, Int. J. Robust Nonlinear Control (2022), doi:10.1002/rnc.6345.

[6] E. Franco, T. Ayatullah, A. Sugiharto, A. Garriga Casanovas, V. Virdyawan, Nonlinear energy-based control of soft continuum pneumatic manipulators, Nonlinear Dyn. 106 (1) (2021a) 229–253, doi:10.1007/s11071-021-06817-1.

[7] E. Franco, A. Garriga Casanovas, J. Tang, F. Rodriguez y Baena, A. Astolfi, Adaptive energy shaping control of a class of nonlinear soft continuum manipulators, IEEE ASME Trans. Mechatron. (2021b) 1–11, doi:10.1109/TMECH.2021.3063121.

[8] E. Franco, F. Rodriguez Y Baena, A. Astolfi, Robust dynamic state feedback for underactuated systems with linearly parameterized disturbances, Int. J. Robust Nonlinear Control 30 (10) (2020) 4112–4128, doi:10.1002/RNC.4985.

[9] I. Gandarilla, V. Santibáñez, J. Sandoval, Control of a self-balancing robot driven by DC motors via IDA-PBC, in: ACM International Conference Proceeding Series, Association for Computing Machinery, New York, New York, USA, 2017, pp. 13–17, doi:10.1145/3149827.3149837.

[10] A. Gheibi, A.R. Ghiasi, S. Ghaemi, M.A. Badamchizadeh, Interconnection and damping assignment control based on modified actor–critic algorithm with wavelet function approximation, ISA Trans. 101 (2020) 116–129, doi:10.1016/j.isatra.2020.01.013.

[11] M.R.J. Harandi, H.D. Taghirad, On the matching equations of kinetic energy shaping in IDA-PBC, J. Frankl. Inst. 358 (16) (2021) 8639–8655, doi:10.1016/j.jfranklin.2021.08.034.

[12] M.C. de Jong, K.C. Kosaraju, J.M. Scherpen, On control of voltage-actuated piezoelectric beam: aKrasovskii passivity-based approach, Eur. J. Control (2022) 100724, doi:10.1016/j.ejcon.2022.100724.

[13] M. Krstic, I. Kanellakopoulos, P. Kokotovic, Nonlinear and Adaptive Control Design, Adaptive and Learning Systems for Signal Processing, Communications and Control, Wiley, 1995.

[14] C. Lv, H. Yu, J. Chen, N. Zhao, J. Chi, Trajectory tracking control for unmanned surface vessel with input saturation and disturbances via robust state error IDA-PBC approach, J. Frankl. Inst. 359 (5) (2022) 1899–1924, doi:10.1016/j.jfranklin.2022.01.036.

[15] A. Mattioni, Y. Wu, H. Ramirez, Y. Le Gorrec, A. Macchelli, Modelling and control of an IPMC actuated flexible structure: a lumped port Hamiltonian approach, Control Eng. Pract. 101 (2020) 104498, doi:10.1016/j.conengprac.2020.104498.

[16] A.D. Mahindrakar, A. Astolfi, R. Ortega, G. Viola, Further constructive results on interconnection and damping assignment control of mechanical systems: the acrobot example, Int. J. Robust Nonlinear Control 16 (14) (2006) 671–685, doi:10.1002/rnc.1088.

[17] K. Nunna, M. Sassano, A. Astolfi, Constructive interconnection and damping assignment for port-controlled Hamiltonian systems, IEEE Trans. Autom. Control 60 (9) (2015) 2350–2361, doi:10.1109/TAC.2015.2400663.

[18] R. Ortega, M. Spong, F. Gomez-Estern, G. Blankenstein, Stabilization of a class of underactuated mechanical systems via interconnection and damping assignment, IEEE Trans. Autom. Control 47 (8) (2002) 1218–1233, doi:10.1109/TAC.2002.800770.

[19] R. Ortega, B. Yi, J.G. Romero, Robustification of nonlinear control systems vis-à-vis actuator dynamics: an immersion and invariance approach, Syst. Control Lett. 146 (2020) 104811, doi:10.1016/j.sysconle.2020.104811.

[20] J.G. Romero, H. Rodríguez-Cortés, Asymptotic stability for a transformed nonlinear UAV model with a suspended load via energy shaping, Eur. J. Control 52 (2020) 87–96, doi:10.1016/j.ejcon.2019.09.002.

[21] M. Ryalat, D.S. Laila, A simplified IDA-PBC design for underactuated mechanical systems with applications, Eur. J. Control 27 (2016) 1–16, doi:10.1016/j.ejcon.2015.12.001.

[22] M. Ryalat, D.S. Laila, H. ElMoaqet, N. Almtireen, Dynamic IDA-PBC control for weakly-coupled electromechanical systems, Automatica 115 (2020) 108880, doi:10.1016/j.automatica.2020.108880.

[23] J. Sandoval, R. Kelly, V. Santibáñez, J. Villalobos-Chin, Energy regulation of torque–driven robot manipulators in joint space, J. Frankl. Inst. 359 (4) (2022) 1427–1456, doi:10.1016/j.jfranklin.2022.01.034.

[24] G. Tao, A simple alternative to the Barbălat lemma, IEEE Trans. Autom. Control 42 (5) (1997) 698, doi:10.1109/9.580878.

[25] R. Wang, C. Zhang, W. Tan, J. Yang, D. Lin, L. Liu, Electroactive polymer-based soft actuator with integrated functions of multi-degree-of-freedom motion and perception, Soft Robot. (2022), doi:10.1089/soro.2021.0104.

[26] Y. Wang, H. Yu, H. Wu, X. Liu, IDA-PBC of the robot manipulator including actuator dynamics, in: Proceedings - 2019 Chinese Automation Congress, CAC 2019, Institute of Electrical and Electronics Engineers Inc., 2019, pp. 5111–5114, doi:10.1109/CAC48633.2019.8996632.

[27] Y.-Q. Yu, L.L. Howell, C. Lusk, Y. Yue, M.-G. He, Dynamic modeling of compliant mechanisms based on the pseudo-rigid-body model, J. Mech. Des. 127 (4) (2005) 760, doi:10.1115/1.1900750.